Ph.D. Thesis

Universitat de Barcelona
Departament de Geodinàmica i Geofísica

A Magnetotelluric Investigation of Geoelectrical Dimensionality and Study of the Central Betic Crustal Structure

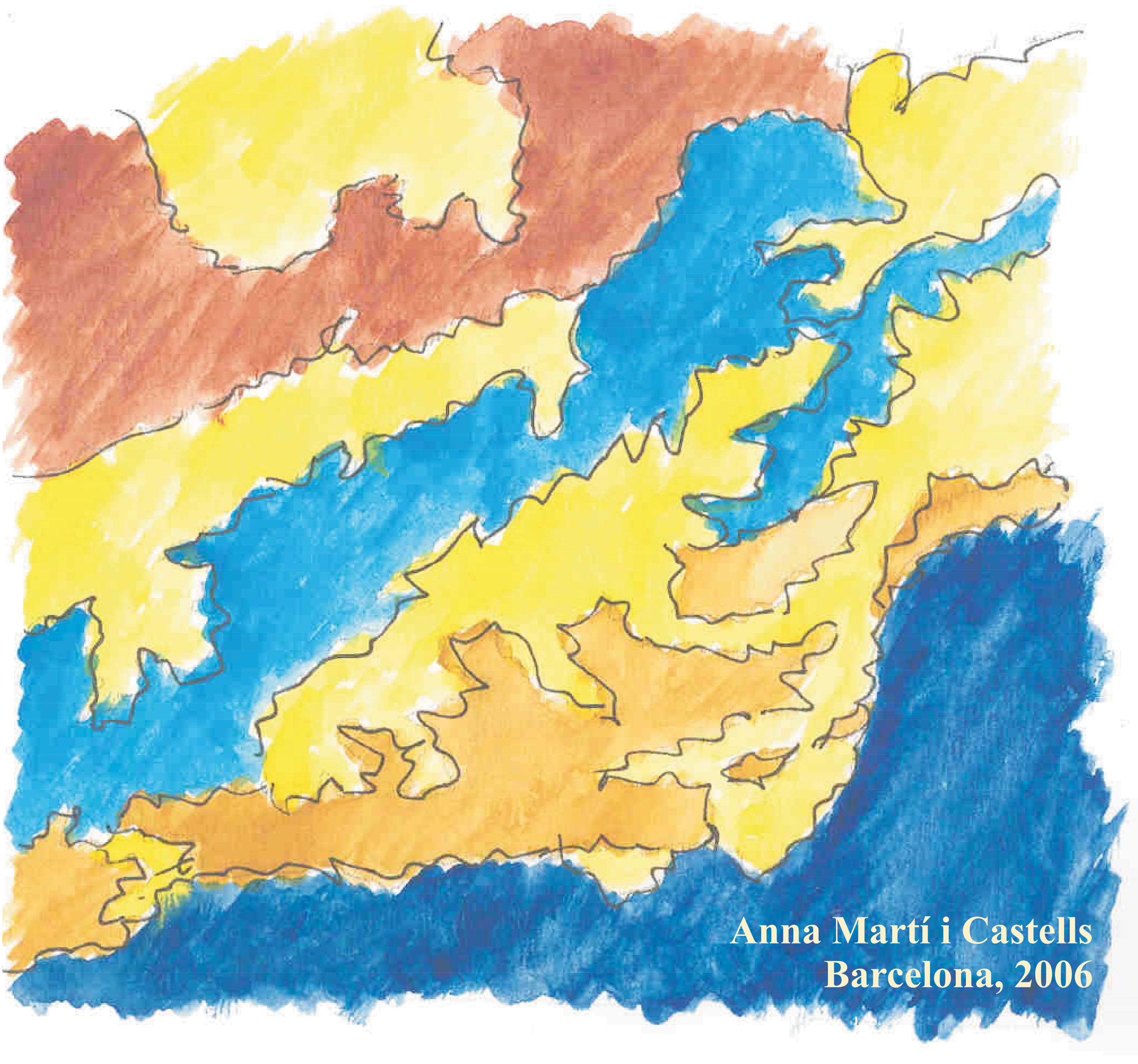

Anna Martí i Castells
Barcelona, 2006

Gràcies…

Finalment puc omplir aquestes darreres pàgines per poder donar les gràcies a totes aquelles persones que heu compartit amb mi aquests anys i heu contribuït a que finalment aquesta tesi s'hagi convertit en una realitat.

Abans que res, agrair sincerament als meus directors, la Pilar Queralt i l'Eduard Roca, per haver-me donat l'oportunitat de realitzar-la, pel temps dedicat, per guiar-me i aconsellar-me, i per tot el que m'heu ensenyat tant de la MT i de la geofísica, com de la geologia.

Gràcies al Juanjo i l'Àlex, pels seus consells, les seves crítiques, i també els seus ànims, que m'han permès aprendre i continuar endavant sabent quina direcció agafar.

Al Jesús Galindo-Zaldívar, del Departamento de Geodinámica de la Universidad de Granada, per col·laborar i participar en la campanya i en totes les idees que ha aportat, i a tota la resta de l'equip que vau aguantar els dies de sol i suor, perquè l'Anna pogués disposar de més dades: la Pilar, la Claudia, la Patricia, el Vicente, el Fernando, el Carlos, l'Antonio i l'Ana. A la Montse Liesa, per aclarir els dubtes petrològics i poder desencallar la interpretació.

A tots aquells amb qui he compartit la oportunitat de formar-me i exercir en la docència: als companys de l'Escola Santa Eulàlia de Cornellà; al Dani, la Trini, l'Eloi i el Pere del grup de física de l'Escola d'Agricultura de la UPC, i als companys de l'Escola Industrial. I als de la UB, amb tantes classes compartides i/o substituïdes amb l'Emma, el Jaume, el Ghia, la Pilar, l'Àlex (també per mentoritzar-me!), la Mireia, el Juanjo, la Berta, la Bea i l'Anna. A tots, per tot el que hem après ensenyant plegats.

A l'Alan G. Jones, per acollir-me a Ottawa i donar-me la oportunitat de treballar amb ell al Geological Survey de Canadà, i endinsar-me una mica més en el món de la MT; també al Jim

Craven, per fer-me sempre un lloc al GSC i convidar-me a participar en els seus projectes, i a la resta de companys del GSC.

Un record molt especial per l'Anna G., amb qui vam començar juntes en el món de la recerca i la geofísica, en els cursos de doctorat, les nostres primeres classes, els projectes de docència, els congressos, per aconsellar-me en tot allò que passa tant dins com fora de la feina, per ser una gran amiga. També a la Bea, entre moltes altres coses, per la teva gran ajuda en les classes, i a la resta de companys del grup de treball, la Claudia, l'Ester, la Mireia, l'Oriol i el Miquel, per les estones bones i no tant bones passades, entre dades, mapes, programes, articles, ajustos i disgustos, formats i deadlines... i també fora d'ell.

A l'Òscar, per ajudar-me en entendre més d'un terme geològic, i per compartir els "fatal errors" del Fortran; i a les noves companyes de despatx, l'Anna C. i la Sara, que també heu viscut el final d'aquesta tesi. Al Gerard i la Wiebke, companys en el món de la MT, per haver-me solucionat algun que altre problema amb el programa dels botonets vermells. I com no, a tots els becaris i becàries del departament de Geodinàmica i Geofísica, pels esmorzars i dinars, que han fet que per una estona ens oblidéssim del que passava a dalt. A l'Héctor, i/o a la comissió de festes i xerinoles, per les escapadetes a la muntanya i pels grans aconteixements gastronòmics. I a la resta de gent del departament, on sempre hi he trobat algú disposat a donar-me un cop de mà.

Als meus pares, per donar-me sempre ànims, i no deixar de sentir-vos orgullosa de mi. Gràcies per deixar-me viure a "Cal Vicencià", per alguna que altra carmanyola furtiva i per les múltiples reparacions. A l'Elena i el David, per estar al meu costat i per comptar amb mi, per les estones passades, i per les rialles. A la iaia Paquita, pels nostres sopars dels dijous, que per molts anys!!!, pels teus consells i històries, i per la teva inesgotable energia, que fa que mai deixi d'admirar-te.

A tots els meus amics i amigues, especialment a la Neus, a l'Anna i l'Emili. A la Marta i el Josep, per les aventures al "pisillu" i per haver viscut de prop els meus nervis i també les alegries, i a tota la colla que ens vam conèixer dalt de l'escenari i que de tant en tant ens trobem al voltant d'una bona taula o fent una llarga passejada per la platja. A l'orquestra de Capellades i als companys del quartet: el Jordi, la Mireia i l'Estefania; als qui més d'un cop he enyorat tot escoltant música mentre intentava fer compilar algun programa.

I a tu, Grant, per estimar-me, escoltar-me i animar-me des de qualsevol costat de l'oceà. Per la teva ajuda en els moments més durs de la tesi, i per fer-me mirar sempre "the whole picture". Gràcies, "language man", per treure tots els "the" de més i canviar tants "make" per "do", i per fer que aquestes línies no necessitin traducció. Per a que puguem escriure el nostre futur plegats.

Masquefa-Vilanova-Ottawa, una llarga
tardor i un molt fred hivern, 2005-06

References

Ábalos, B., Carreras, J., Druguet, E., Escuder Viruete, J., Gómez Pugnaire, M.T., Lorenzo Alvárez, S., Quesada, C., Rodríguez Fernández, L.R. and Gil-Ibarguchi, J.I. (coordinator), 2002. Variscan and Pre-Variscan Tectonics. *In:* Gibbons, W. and Moreno, T. (eds) The Geology of Spain, *Geological Society (London)*, 155-183.

Arango, C., 2005. Estudio Magnetotelúrico de la zona de Lluchmajor (Mallorca): Avances en el proceso de datos y modelo 3D, PhD Thesis, *Departament de Geodinàmica i Geofísica, Universitat de Barcelona*.

Ardizone, J., Mezcua, J. and Socias, I. 1989. Mapa aeromagnético de la España Peninsular, *Instituto Geográfico Nacional*, Madrid.

Azañón J.M., and Crespo-Blanc, A., 2000. Exhumation during a continental collision inferred from the tectonometamorphic evolution of the Alpujarride Complex in the central Betics (Alboran Domain, SE Spain), *Tectonics*, **19**, 549-565.

Azañón, J. M., Galindo-Zaldívar, J., García-Dueñas, V. and Jabaloy, A., 2002. Alpine Tectonics II: Betic Cordillera and Balearic Islands. *In*: Gibbons, W. and Moreno, T. (eds) The Geology of Spain, *Geological Society (London)*, 401-416.

Babu, J.K. and Singh, K., 1983. Inference on means using the bootstrap, *Annals of Statistics*, **11**, 999-1003.

Bahr, K., 1988. Interpretation of the magnetotelluric impedance tensor: regional induction and local telluric distortion, *J. Geophys.*, **62**, 119-127.

Bahr, K., 1991. Geological noise in magnetotelluric data: a classification of distortion types, *Phys. Earth planet. Inter.,* **66**, 24-38.

Balanyá, J.C. and García-Dueñas, V., 1987. Les directions structurales dans le Domaine d'Alborin de part et d'autre du Detroit de Gibraltar. *Comptes Rendus de l'Academie des Sciences de Paris*, **304**, 929-932.

Banda, E. and Ansorge, J., 1980. Crustal structure under the central and eastern part of the Betic Cordillera, *Geophys. J.R. Astron. Soc.,* **63**, 515-532.

Banda, E., Udias, A., Mueller, St., Mezcua, J., Boloix, M., Gallart, J., and Aparicio, A., 1983. Crustal structure beneath Spain from deep seismic sounding experiments. *Physics of the Earth and Planetary Interiors,* **31**, 277-280.

Banda, E., Gallart, J., García-Dueñas, V., Dañobeitia, J.J. and Makris, J., 1993. Lateral variation of the crust in the Iberian Peninsula, New evidence from the Betic Cordillera, *Tectonophysics*, **221**, 53-66.

Banks, C.J. and Warburton, J., 1991. Mid crustal detachment in the Betic system of southeast Spain, *Tectonophysics*, **191**, 275-289.

Barranco, L., Ansorge, J. and Banda, E., 1990. Seismic refraction constraints on the geometry of the Ronda peridotitic massif (Betic Cordilera, Spain), *Tectonophysics*, **184**, 379-392.

Bendat, J.S. and Piersol, A.G., 1971. Measurement and Analysis of Random Data, *John Wiley and Sons*, New York.

Berdichevsky, M.N. and Dmitriev, V.I., 1976. Basic principles of interpretation of magnetotelluric curves, in *Geoelectric and Geothermal Studies*, pp. 165-221, ed. Á. Ádam, *KAPG Geophysical Monograph*, Akademiai Kaido, Budapest.

Bohoyo F., Galindo-Zaldivar J. and Serrano I., 2000. Main features of the basic rock bodies of the Archidona Region derived from geophysical data (External Zones, Betic Cordillera), *Comptes Rendus de l'Academie des Sciences. Series IIA: Earth and Planetary Science*, **330** (10), 667-674.

Bostick, F.X., 1977. A Simple Almost Exact Method of MT Analysis, *Workshop on Electrical Methods in Geothermal Exploration*, Snowbird, Utah: U.S. Geological Survey Contract 14-08-001-6-359.

Braga J.C., and Martín, J.M., 1987. Sedimentación cíclica lagunar y bioconstrucciones asociadas en el Trías superior alpujarride, *Cuadernos Geología Ibérica*, **11**, 459-473.

Brigham, E.O., 1974. The Fast Fourier Transform, *Prentice-Hall, Inc*.

Brown, C. 1994. Tectonic interpretation of regional conductivity anomalies. Surveys in *Geophysics*, **15**, 123 - 157.

Cagniard, L., 1953. Basic theory of the magnetotelluric method of geophysical prospecting, *Geophysics*, **18**, 605-635.

Caldwell, T.G., Bibby, H.M. and Brown, C., 2004. The Magnetotelluric Phase Tensor, *Geophys. J. Int.,* **158**, 457-469.

Calvert, A., Sandvol, E., Seber, D., Barazangi, M., Roecker, S., Mourabit, T., Vidal, F., Alguacil, G., and Jabour, N., 2000. Geodynamic Evolution of the Lithosphere and Upper Mantle Beneath the Alboran Region of the Western Mediterranean: Constraints from Travel Time Tomography, *Journ. Geophys. Res.*, **105**, 10871-10898.

Campbell, W.H., 2003. Introduction to Geomagnetic Fields. *Cambridge University Press*.

Cantwell, T., 1960. Detection and analysis of low frequency magnetotelluric signals. Ph.D. Thesis, *Dept. of Geology and Geophysics, M.I.T. Cambridge, MA*.

Carbonell, R., Sallarés, V., Pous, J., Dañobeitia, J.J., Queralt, P., Ledo, J.J. and García-Dueñas, V., 1998. A multidisciplinary study in the Betic Chain. *Tectonophysics*, **288**, 137-152.

Casas, A. and Carbó, A., 1990. Deep structure of the Betic Cordillera derived from the interpretation of a complete Bouguer anomaly map, *Journal of Geodynamics*, **12**, 137-147.

Chave, A.D. and Smith, J.T., 1994. On electric and magnetic galvanic distortion tensor decompositions, *J. Geophys. Res.*, **99**, B3, 4669-4682.

Chave A.D. and Thomson D.J., 2004. Bounded influence magnetotelluric response function estimation. *Geophysical Journal International*, **157**, 988-1006.

Constable, S.C., Orange, A.S., Hoversten, G.M. and Constable, C.G., 1987. Occam's inversion: A practical algorithm for generating smoth models from EM sounding data, *Geophysics*, **63**, 816-825.

Cook, F.A. and Jones, A.G., 1995. Seismic reflections and electrical conductivity: A case of Holmes's curious dog?, *Geology*, **23** (2), 141-144.

Dañobeitia, J.J., Sallarès, V. and Gallart, J., 1998. Local earthquakes seismic tomography in the Betic Cordillera (southern Spain), *Earth and Planetary Science Letters*, **160**, 225-239.

Davis, G.H. and Reynolds, S.J., 1996. Structural Geology of Rocks and Regions, 2nd ed., *Wiley and Sons*, NY.

Dewey, J.F., Pitman III, W.C., Ryan, W.B.F. and Bonnin, J., 1973. Plate Tectonics and the evolution of the Alpine system. *Geol. Soc. Amer. Bull.,* **84**, 3137-3180.

Dewey, J.F., Helman, M.L., Turco, E., Hutton, D.H.W. and Knott, S.D., 1989. Kinematics of the western Mediterranean. In: Coward M.P., Dietrich, D. and Park, R.G. (eds), Alpine Tectonics, *Geol. Soc. Spec. Publ.*, **45**, 265-283.

Doglioni, C., Fernàndez, M., Gueguen, E. and Sabat, F., 1999. On the interference between the early Apennines-Maghrebides backarc extension and the Alps-Betics orogen in the Neogene Geodynamics of the Western Mediterranean, *Boll. Soc. Geol. It.*, **118**, 75-89.

Dupis, A., 1997. 1961-1994: A third of a century of magnetotellurics, *The leading Edge*, **16**, 497-502.

Efron, B., 1979. Bootstrap methods: Another look at the jackknife. *Annals of Statistics,* **7**, 1-26.

Efron, B. and Tibshirani, R. J., 1998: An introduction to the bootstrap. *Monographs on statistics and applied probability*, **57**, Boca Raton, CRC, 436 pp.

Egbert, G.D. and Booker, J.R., 1986. Robust estimation of geomagnetic transfer functions. *Geophys. J. R. Astron. Soc.,* **87**, 173-194.

Favre, P. and Stampfli, G., 1992. From rifting to passive margin: the example of the Red Sea, Central Atlantic and Alpine Tethys, *Tectonophysics*, **215**, 67-97.

Fernàndez, M., Berástegui, X., Puig,C. García-Castellanos, D., Jurado, M.J., Torné, M. and Banks, C., 1998a. Geophysical and geological constraints on the evolution of the Guadalquivir foreland basin, Spain. In: Mascle, A., Puigdefabregas, C., Fernàndez, M. (eds), *Cenozoic foreland Basins of western Europe*, *Geol. Soc. Spec. Publ*, **134**, 29-48.

Fernàndez, M., Marzán, I., Correia, A. and Ramalho, E., 1998b. Heat flow, heat production, and lithospheric thermal regime in the Iberian Peninsula. Tectonophysics, **291**, 29-54.

Fischer, G. and Masero, W., 1994. Rotational properties of the magnetotelluric impedance tensor, the example of the Araguainha impact crater, Brazil, *Geophys. J. Int*., **119**, 548-560.

Friedrichs, B., 2003. Mapros, Magnetotelluric Processing Software (Metronix) User Manual.

Frizon de Lamotte, D., A. Crespo-Blanc, B. Saint-Bezar, M. Fernàndez, H. Zeyen, and Ayarza, P., 2004. TRANSMED-TRANSECT I [Betics, Alboran Sea, Rif, Moroccan Meseta, High Atlas, Jbel Saghro, Tindouf basin], edited by R. W. Cavazza, F., Spakman, W., Stampfli, G. and Ziegler, P.A., *Springer-Verlag*.

Galindo-Zaldívar, J., Jabaloy, A., González-Lodeiro, F. and Aldaya, F., 1997. Crustal structure of the central sector of the Betic Cordillera (SE Spain), Tectonics, **16** (1), 18-37.

Galindo-Zaldívar, J., González-Lodeiro, F. and Vera, J.A., 2004. Datos de Geología de Subsuelo y relaciones con otros dominios geológicos españoles. In: Geología de España, J.A. Vera, editor, *SGE-IGME*, Madrid, 350-352.

Gamble, T.D., Goubau, W.M. and Clarke, J., 1979. Magnetotellurics with a remote magnetic reference, *Geophysics*, **44**, 53-68.

Garcia, X., Chave, A.D. and Jones, A.G., 1997. Robust processing of magnetotelluric data from the auroral zone, *J. Geomagn. Geoelectr.*, **49**, 1451-1468.

García, X. and Jones, A.G., 1999. Extended decomposition of MT data, in The second international symposium on Three-dimensional Electromagnetics (3DEM-2), Salt Lake City (USA), 27-29 October.

García-Hernández, M., López-Garrido, A.C., Rivas, P., Sanz de Galdeano, C. and Vera, J., 1980. Mesozoic paleogeographic evolution in the External Zones of the Betic Cordillera (Spain), *Geol. Mijnb*, **59**, 155-168.

García-Dueñas, V., Martínez-Martínez, J.M., Soto, J.I., 1988. Los Nevado-Filabrides, una pila de pliegue-mantos separados por zona de cizalla, *II Cong. geol. España*, 17-26.

García-Dueñas, V., Balanyá, J.C. and Martínez-Martínez, J., 1992. Miocene extensional detachment in the outcropping basement of the Northern Alboran basin (Betics) and their tectonic implications, *Geo-Mar. Lett.,* **12**, 88-95.

García-Dueñas, V., Banda, E., Torné, M., Córdoba, D. and ESCi-Béticas Working Group, 1994. A deep seismic reflection survey across the Betic Chain (southern Spain): first results, *Tectonophysics*, **232**, 77-89.

Groom, R.W. and Bailey, R.C.,1989. Decomposition of the magnetotelluric impedance tensor in the presence of local three-dimensional galvanic distortion, *J. Geophys. Res.,* **94**, 1913-1925.

Gutsher, M.A., Malod, J., Rehault, J.P., Contrucci, I., Klingelhoefer, F., Mendes-Victor, L. and Spakman, W., 2002. Evidence for active subduction beneath Gibraltar, *Geology*, **30**, vol. 12, 1071-1074.

Hjelt, S.E. and Korja, 1993. Lithospheric and upper-mantel structures, results of electromagnetic sounding in Europe, *Physics of the Eaarth and Planetary Interiors*, **79**, 137-177.

Huber. P.J., 1981. Robust Statistics, *Wiley*, New York.

IGN, 1976. Mapa de anomalías de Bouguer. Escala 1:500000. Madrid.

IGN, 2001. Catalogo Sísmico Nacional.

Jabaloy, A., Fernández-Fernández, E.M., González-Lodeiro, F. and Sanz de Galdeano, C. 2005. The structure of the Eastern Betic Cordillera (SE Spain), *Joint Earth Science Meeting*, France.

Jiracek, G., 1990. Near-surface and topographic distortions in electromagnetic induction. *Surv. Geophys*., **11**, 163-203.

Jolivet, L. and Faccenna, C., 2000. Mediterranean extension and the Africa-Eurasia collision, *Tectonics*, **19** (6), 1095-1106.

Jones, A.G. and Jödicke, H., 1984. Magnetotelluric transfer function estimation improvement by a coherence-based rejection technique, 54th Annual International Meeting, *Society of Exploration Geophysicists*, Atlanta, Dec. 2-6, 1984.

Jones, A.G., 1988. Static Shift of Magnetotelluric Data and its Removal in a Sedimentary Basin Environment, *Geophysics*, **53**, 967-978.

Jones, A.G., Chave, A.D., Egbert. G., Auld, D. and Bahr, K., 1989. A comparison of Techniques for Magnetotelluric Response Function Estimation. *Journal of Geophysical Research*, **94**, 14210-14213.

Jones, A.G., 1992. Electrical Conductivity of the Continental Lower Crust. *In:* Continental Lower Crust, edited by D.M. Fountain, R.J. Arculus and R.W. Kay, *Elsevier*, 81-143.

Jones, A.G., 1993. The COPROD2 dataset: Tectonic setting, recorded MT data and comparison of models, *J. Geomag. Geoelect*r., **45**, 933-955.

Jones, A.G. and Groom, R.W., 1993. Strike angle determination from the magnetotelluric impedance tensor in the presence of noise and local distortion: rotate at your peril!. *Geophys. J. Int.,* **113,** 524-534.

Jones, A.G., Groom, R.W. and Kurtz, R.D., 1993. Decomposition and Modelling of the BC87 dataset, *J. Geomag. Geoelectr.*, **45**, 1127-1150.

Jones, A.G., J. Ledo and I.J. Ferguson, 2005. Electromagnetic images of the Trans-Hudson orogen: The North American Central Plains (NACP) anomaly revealed, *Canadian Journal of Earth Sciences*, **42**, 457-478.

Jones, F.W., Munro, R.A., Craven, J.A., Boerner, D.E., Kurtz, R.D. and Sydora, R.D., 2002. Regional geoelectrical complexity of the Western Canada Basin from magnetotelluric tensor invariants, *Earth Planets Space*, **54**, 899-905.

Junge, A, 1996: Characterization of and Correction for Cultural Noise, *Surveys in Geophysics*, **17**, 361-391.

Kaufman, A.A. and Keller, G.V., 1981. The Magnetotelluric Sounding Method, *Methods in Geochemistry and Geophysics*, **15**. Amsterdam.

Kaufman, A. A., 1988. Reduction of the geological noise in magnetotelluric soundings, *Geodex*, **25**, 145-161.

Keller, G.V. and Frischkenecht, F.C., 1966. Electrical Methods in Geophysical Prospeting, *International Series in Electromagnetic Waves*, vol. **10**, Pergamon Press.

Keller, G.V., 1987. Rock and Mineral Properties. *In:* Electromagnetic Methods in Applied Geophysics – Vol 1. Theory. *Soc. Expl. Geophys.,* Tulsa, OK.

Kiss, J., Szarka, L. and Prácser, E., 2005. Second-order magnetic phase transition in the Earth *Geophysical Research Letters*, **32**, L24310, doi:10.1029/2005GL024199.

Larsen, J., 1977. Removal of local surface conductivity effects from low frequency mantle response curves, *Geodinamica Acta*, **12**, 183-186.

Ledo, J., 2005. 2-D versus 3-D magnetotelluric data interpretation, *Surveys in Geophysics*, **26**, 671-806.

Ledo, J.J., Queralt, P. and Pous, J., 1998. Effects of galvanic distortion on magnetotelluric data over a three dimensional structure, *Geophys. J. Int.*, **132**, 295-301.

Ledo, J., Gabàs, A. and Marcuello, A., 2002a. Static shift levelling using geomagnetic transfer functions. *Earth Planets Space*, **54**, 493-398.

Ledo, J., Queralt, P., Martí, A. and Jones, A.G., 2002b. Two-dimensional interpretation of three-dimensional magnetotelluric data: an example of limitations and resolution, *Geophys. J. Int.*, **150**,127-139.

Ledo, J., Jones, A.G., Ferguson, I.J. and Jones, A.G., 2004. Lithospheric structure of the Yukon, northern Canada Cordillera, obtained from magnetotelluric data, *Journal of Geophysical Research*, **119**, B04410, DOI 10.1029/2003JB002516.

Lezaeta, P., 2002. Confidence limit of the magnetotelluric phase sensitivity skew, *Earth Planets Space*, **54**, 451-457.

Lilley, F.E.M., 1976. Diagrams for magnetotelluric data, *Geophysics*, **41**, 766-770.

Lilley, F.E.M., 1993: Magnetotelluric analysis using Mohr circles, *Geophysics*, **58,** 1498-1506.

Lilley, F.E.M., 1998a: Magnetotelluric tensor decomposition: 1. Theory for a basic procedure, *Geophysics*, **63,** 1884-1897.

Lilley, F.E.M., 1998b: Magnetotelluric tensor decomposition: 2. Examples of a basic procedure, *Geophysics*, **63,** 1898-1907.

Lonergan, L. and White, N., 1997. Origin of the Betic-Rif mountain belt, *Tectonics*, **16**, 504-522.

López Ruiz, J. (coord), Cebrià, J.M., Doblas, M. and Benito, R. 2004: La región volcánica de Almería-Murcia. En: Geología de España (J.A. Vera, Ed.), *SGE-IGME*, Madrid, 678-682.

Lupton, R. H., 1993. Statistics in Theory and Practice, *Princeton University Press*.

Mackie, R.L. and Madden, T.R., 1993. Three-Dimensional Magnetotelluric Inversion using Conjugate Gradients, *Geophys. J. Int.,* **115**, 215-229.

Mackie, R.L., Madden, T.R., and Wannamaker, P. E., 1993. Three-dimensional magnetotelluric modeling using difference equations – Theory and comparisons to integral equations solutions, *Geophysics*, **58**, 215-226.

Mackie, R., Rieven, S. and Rodi, W., 1997. Users Manual and Software Documentation for Two-Dimensional Inversion of Magnetotelluric Data, *GSY-USA Inc. San Francisco* (USA).

Malan, D.J., 1963. Physics of lightning. *English Universities Press. London.*

Mareschal, M., Fyfe, W.S., Percival, J. and Chan, T., 1992. Grain-boundary graphite in Kapuskasing gneisses and implications for lower-crustal conductivity, *Nature*, **357**, 674-676.

Marquis, G., Jones, A.G. and Hyndman, R.D, 1995. Coincident conductive and reflective lower crust across a thermal boundary in southern British Columbia, Canada, *Geophys. J. Int*., **120**, 111-131.

Martí, A., Queralt, P. and Roca, E., 2004. Geoelectric dimensionality in complex geologic areas: application to the Spanish Betic Chain. *Geophys. J. Int.*, **157**, 961-974.

Martí, A., Queralt, P., Jones, A.G. and Ledo, J., 2005. Improving Bahr's invariant parameters using the WAL approach, *Geophys. J. Int.,* **163**, 38-41.

Mazzoli, S. and Helman, M., 1994. Neogene patterns of relative plate motion for Africa-Europe: some implications from recent Mediterranean tectonics, *Geol. Rund.*, **83**, 464-468.

McNeice, G and Jones, A.G., 2001. Multisite, multifrequency tensor decomposition of magnetotelluric data, *Geophysics*, **66**, 158-173.

McPherron, R.L., 2005. Magnetic pulsations: their sources and relation to solar wind and electromagnetic activity, *Surveys in Geophysics,* **26** (5), 546-592.

Medialdea, T., Suriñach, E., Vegas, R., Banda, E. and Ansorge, J., 1986. Crustal structure under the western end of the betic Cordillera (Spain), Ann. Geophys., **4** (B4), 457-464.

Meju, M.A., 2005. Simple relative space–time scaling of electrical and electromagnetic depth sounding arrays: implications for electrical static shift removal and joint DC-TEM data inversion with the most-squares criterion, *Geophysical Prospecting*, **53**, 463-479.

Monié, P., Galindo-Zaldívar, J., González Lodeiro, F., Goffe, B. and Jabaloy, A., 1991. 40Ar/39Ar geochronology of Alpine tectonism in the Betic Cordilleras (southern Spain), *Journal of the Geological Society*, London, **148**, 289-297.

Morales, J., Serrano, I., Jabaloy, A., Galindo-Zaldívar, J., Zhao, D., Torcal, F., Vidal, F., and González-Lodeiro, F., 1999. Active continental subduction beneath the Betic Cordillera and the Alborán Sea, *Geology*, **27**, 735-738.

Muñoz, G., 2005. Estudi Magnetotel·lúric tridimensional de les estructures varisques del SW de la Península Ibèrica, PhD Thesis, *Departament de Geodinàmica i Geofísica*, *Universitat de Barcelona*.

Navarro-Vilá, F. and García-Dueñas, V., 1980. Geological map, Sheet La Peza 1010, *Instituto Geológico y Minero de España*, Madrid, scale 1:50000.

Newman, G.A, and Alumbaugh, D.L., 2000. Three-Dimensional Magnetotelluric Inversion using Non-Linear Conjugate Gradients, *Geophys. J. Int.*, **140**, 410-424.

Nover, G., 2005. Electrical Properties of Crustal and Mantle Rocks – A Review of Laboratory Measurements and their Explanation, *Surveys in Geophysics*, **26** (5), 593-651.

Ogawa, Y., 2002. On two-dimensional modeling of magnetotelluric field data. *Surveys in Geophysics*, **23**, 99-273.

Padilha, A.L., 1999. Behaviour of magnetotelluric source fields within the ecuatorial zone, *Earth Planets Space*, **51**, 1119-1125.

Palacky, G.J., 1987. Resistivity Characteristics of Geologic Targets. *In:* Electromagnetic Methods in Applied Geophysics – Vol 1. Theory. *Soc. Expl. Geophys.,* Tulsa, OK.

Park, S.K. and Mackie, R.L., 2000. Resistive (dry?) lower crust in an active orogen, Nanga Parbat, northern Pakistan, *Tectonophysics*, **316**, 359-380.

Pedersen, L.B. and Engels, M., 2005. Routine 2D inversion of magnetotelluric data using the determinant of the impedance tensor, *Geophysics*, **70**, G33-G41.

Pek, J. and Verner, T., 1997. Finite-difference modelling of magnetotelluric fields in two-dimensional anisotropic media, *Geophys. J. Int.,* **128**, 505-521.

Pérez-Estaún, A. and Bea, F. (Eds.), 2004. Macizo Ibérico, en: Geología de España (J.A. Vera, Ed.), *SGE-IGME*, Madrid, 19-230.

Pirjola, R., 1992. On magnetotelluric source effects caused by an auroral electrojet system, *Radio Sci.*, **27**, 463-468.

Platt, J.P. and Vissers, R.L.M., 1989. Extensional collapse of thickered continental lithosphere: A working hypothesis for the Alboran Sea and Gibraltar arc, *Geology*, **17**, 540-543.

Platt, J.P., Allerton, S., Kirker, A., Mandeville, C., Mayfield, A., Platzman, E.S. and Rimi, A., 2003. The ultimate arc: differential displacement, oroclinal bending and vertical axis rotation in the External Betic-Rif arc, *Tectonics*, **22** (3), DOI 10.10292001TC001321.

Polyak, B.G., Fernàndez, M., Khutorskoy, M.D., Soto, J.I., Basov, I.A., Comas, M.C., Ye. Khain, V., Alonso, B., Agapova, G.V., Mazurova, I.S., Negredo, A., Tochitsky, V.O., de la Linde, J., Bogdanov N.A. and Banda, E., 1996. Heat flow in the Alboran Sea (the western Mediterranean), *Tectonophysics*, **263**, 191-218.

Pous, J., Queralt, P., Ledo, J.J. and Roca, E., 1999. A high electrical conductive zone at lower crustal depth beneath the Betic Chain (Spain), *Earth and Planetary Science Letters*, **167**, 35-45.

Press, W.H., Flannery, B.P., Teukolsky, S.A., Vetterling, W.T., 1992. Numerical Recipes in Fortran: The Art of Scientific Computing, *Cambridge University Press*.

Radhakrishnamurty, C. and Likhite, S.D., 1970. Hopkinson effect, blocking temperature and Curie point in basalts, *Earth and Planetary Science Letters*, **7***, 389-396.*

Rehault, J.P., Boillot, G. and Mauffret, A., 1984. The western Mediterranean Basin, geological evolution, *Mar. Geol.,* **55**, 447-477.

Romo, J.M., Gomez-Treviño, E. and Esparza, F.J., 1999. An invariant representation of the magnetic transfer function in magnetotellurics, *Geophysics*, **64**, 1418-1428.

Rosenbaum, G., Lister, G.S., and Duboz, C., 2002. Relative motions of Africa, Iberia and Europe during Alpine orogeny, *Tectonophysics*, **359**, 117-129.

Royden, L.H., 1993. Evolution of retreating subduction boundaries formed during continental collision, *Tectonics*, **12**, 629-638.

SAMTEX (Southern African Magnetotelluric Experiment) Workshop on MT data Processing. Dublin Institute of Advanced Physics. March 2004.

Sanz de Galdeano, C. and Vera, J.A., 1992. Stratigraphic record and palaeogeographical context of the Neogene basins in the Betic Cordillera, Spain, *Basin Research*, **4**, 21-36.

Sasaki, Y., 2001. Full 3-D Inversion of Electromagnetic Data on PC, *J. Appl. Geophys.,* **46**, 45-54.

Schettino, A. and Scotese, C. 2002. Global kinematic constraints to the tectonic history of the Mediterranean region and surrounding areas during the Jurassic and Cretaceous. *In:* Rosenbaum, G. and Lister, G. S., Reconstruction of the evolution of the Alpine-Himalayan orogeny, *Journal of the Virtual Explorer*.

Schwalenberg, K., Rath, V. and Haak, V., 2002. Sensitivity studies applied to a two-dimensional resistivity model from the Central Andes, *Geophys. J. Int.,* **150**, 673-686.

Seber, D., Barazangi, M., Ibenbrahim, A. and Demnati, A., 1996. Geophysical evidence for lithospheric delamination beneath the Alboran Sea and Rif-Betics mountains, *Nature*, **379**, 785-790.

Serrano, I., Bohoyo-Muñoz, F., Galindo-Zaldivar, J., Morales-Soto, J., Zhao, D. P., 2002. Geophysical signatures of a basic-body rock placed in the upper crust of the external zones of the Betic Cordillera (Southern Spain), *Geophysical Research Letters*, **29** (11).

Serrano, I., Morales, J., Zhao, D., Torcal, F. and Vidal, F., 1998. P-wave tomographic images in the Central Betics-Alborán sea (South Spain) using local earthquakes: contribution for a continental collision, *Geophysical Research Letters*, **25** (21), 4031-4034.

Simpson, F. and Bahr, K., 2005. Practical Magnetotellurics, *Cambridge Univesity Press*.

Sims, W.E., Bostick, F.X.Jr. and Smith, H.W., 1971. The estimation of magnetotelluric impedance tensor from measured data, *Geophysics*, **36**, 938-942.

Siripunvaraporn, W. and Egbert, G., 2000. An efficient data-subspace inversion method for 2-D magnetotelluric data, *Geophysics*, **65**, 3, 791-803.

Siripunvaraporn, W., Egbert, G., Lenbury, Y. and Uyeshima, M., 2005. Three-dimensional magnetotelluric inversion: data-space method, *Physics of the Earth and Planetary Interiors*, **150**, 3-14.

Smith, J.T. and Booker, J., 1991. Rapid inversion of two- and three-dimensional magnetotelluric data, *J. Geophys. Res*., **96**, 3905-3922.

Smith, J.T., 1995. Understanding telluric distortion matrices, *Geophys. J. Int*., **122**, 219-226.

Suriñach, E. and Udías, A., 1978. Determinación de la raíz de Sierra Nevado-Filabres a partir de sondeos sísmicos profundos y medidas gravimétricas. *In:* Geodinámica de la Cordillera Bética y Mar de Alborán, *Univ. de Granada*, 25-34.

Swift, C.M., 1967. Magnetotelluric investigation of an electrical conductivity anomaly in the southwestern United States, *PhD thesis*, Department of Geology and Geophysics, MIT, Cambridge, MA (reprinted in *Magnetotelluric Methods*, pp. 156-166, ed. Vozoff, K., Geophys. Reprint Ser. No. 5. 1988, SEG, Tulsa, OK).

Szarka, L. and Menvielle, M., 1997. Analysis of rotational invariants of the magnetotelluric impedance tensor, *Geophys. J. Int.,* **129**,133-142.

Szarka, L., 1999. A correction to Bahr's "phase deviation" method for tensor decomposition. *Earth Planets Space*. **51**, 1019-1022.

Thompson, A.B., 1992. Metamorphism and Fluids. *In*: Understanding the Earth, eds. Brown, G.C., Hawkesworth, C.J. and Wilson, R.C.L., *Cambridge University Press*.

Thomson, D.J. and Chave, A.D., 1991. Jackknifed error estimates for spectra, coherences, and transfer functions. *In: Advances in spectrum analysis and array processing* (Shykin, S., ed.), pp 58-113, Englewood Cliffs, NJ: Prentice Hall.

Tikhonov, A.N., 1950. Determination of the electrical characteristics of the deep strata of the Earth's crust, *Dokl. Akad. Nauk.* SSSR, **73**, 295-297.

Torné, M. and Banda, E., 1992. Crustal thinning from the Betic Cordillera to the Alboran Sea, *Geo-Marine Letters*, **12**, 76-81.

Torné, M., Fernàndez, M., Comas, M.C. and Soto, J.I., 2000. Lithospheric structure beneath the Alboran Basin: Results from 3D gravity modeling and tectonic relevance, *Journal of Geophysical Research*, **105**, 3209-3228.

Tournerie, B., Chateau, M. and Marceotte, D., 2004. Estimation and removal of the MT static shift effect using geostatistical methods, *17th International Workshop on Electromagnetic Induction in the Earth.* Hyderabad (India).

Trad, D.O. and Travassos, J.M., 2000. Wavelet filtering of magnetotelluric data, *Geophysics*, **65**, 482-491.

Utada, H. and Munekane, H., 2000. On galvanic distortion of regional three-dimensional magnetotellurics impedances, *Geophys. J. Int.*, **140**, 385-398.

Vera, J.A. (Ed.), 2004. Cordillera Bética y Baleares, en: Geología de España (J.A. Vera, Ed.), *SGE-IGME*, Madrid, 19-230. 347-464.

Vozoff, K., 1972. The magnetotelluric method in the exploration of sedimentary basins, *Geophysics*, **37**, 98-141.

Vozoff, K. 1991. The magnetotelluric method. *In:* Electromagnetic Methods in Applied Geophysics – Vol 2. Applications. *Soc. Expl. Geophys.,* Tulsa, OK.

Wannamaker, P.E., Hohmann, G.W. and Ward, S.H., 1984. Magnetotelluric responses of three-dimensional bodies in layered earths, *Geophysics*, **49**, 1517-1533.

Wannamaker, P. E., Stodt, J.A. and Rijo, L., 1987. A stable finite element solution for two-dimensional magnetotelluric modelling, *Geophys. J. R. Astr. Soc.,* **88**, 277-796.

Wannamaker, P.E., 1999. Affordable magnetotellurics: Interpretations in natural environments, in Three-Dimensional Electromagnetics, eds Oristaglio, M. and Spies, B., *Society of Exploration Geophysicists*, Tulsa.

Weaver, J.T., Agarwal, A.K. and Lilley, F.E.M., 2000. Characterisation of the magnetotelluric tensor in terms of its invariants, *Geophys. J. Int.,* **141**, 321-336.

Weaver, J.T., Agarwal, A.K. and Lilley, F.E.M., 2003. The relationship between the magnetotelluric tensor invariants and the phase tensor of Caldwell, Bibby and Brown, *3DEMIII Workshop*, Adelaide.

Wight, D.E. and Bostick, F.X., 1980. Cascade decimation – A technique for real time estimation of power spectra, Proc. IEEE Intern. Conf. Acoustic, Speech, Signal Processing, Denver, Colorado, April 9-11, 626-629.

Zappone, A., Fernàndez, M., García-Dueñas, V. and Burlini, L., 2000. Laboratory measurements of seismic P-wave velocities on rocks from the Betic chain (southern Iberian Peninsula), *Tectonophysics*, **317**, 259-272.

Zhang, P., Roberts, R.G. and Pedersen, L.B., 1987. Magnetotelluric Strike Rules, *Geophysics*, **52**, 267-278.

Zhang,Y. and Paulson, K.V., 1997. Enhancement of signal-to-noise ratio in natural source transient magnetotelluric data with wavelet transform. *Pure and Applied Geophysics*, **149**, 405-419.

Zhdanov, M.S., Fang, S. and Hursan, G., 2000. Electromagnetic Inversion using Quasi-Linear Approximation, *Geophysics*, **65**, 1501-1513.

Zonge, K.L. and Hughes, L.J., 1991. Controlled Source audio-frequency magnetotellurics. *In:* Electromagnetic Methods in Applied Geophysics-Vol 2. Applications. *Soc. Expl. Geophys.,* Tulsa, OK.

Appendix A: Expressions of the Errors of WAL Invariants and Strike Angles using Classical Error Propagation

To obtain the analytical expression of the errors (δI_k) of each invariant (I_k), classical error propagation was applied to equations (2.10 to 2.18), regarding the errors of the tensor components M_{ij} as statistically independent. The expressions are shown in terms of ξ_i and η_i (see eq. 2.8) and their errors:

$$\zeta_1 = \xi_1 + \eta_1 i = \frac{M_{xx} + M_{yy}}{2}, \tag{A.1a}$$

$$\zeta_2 = \xi_2 + \eta_2 i = \frac{M_{xy} + M_{yx}}{2}, \tag{A.1b}$$

$$\zeta_3 = \xi_3 + \eta_3 i = \frac{M_{xx} - M_{yy}}{2}, \tag{A.1c}$$

$$\zeta_4 = \xi_4 + \eta_4 i = \frac{M_{xy} - M_{yx}}{2}. \tag{A.1d}$$

Since $\delta(\mathrm{Re}\, M_{ij}) = \delta(\mathrm{Im}\, M_{ij}) = \delta(M_{ij}) = (\mathrm{var}(M_{ij}))^{1/2}$ (eq. 3.1):

$$\delta\xi_1 = \delta\xi_3 = \delta\eta_1 = \delta\eta_3 = \frac{1}{2}\sqrt{\left(\delta M_{xx}\right)^2 + \left(\delta M_{yy}\right)^2}\ , \tag{A.2a}$$

$$\delta\xi_2 = \delta\xi_4 = \delta\eta_2 = \delta\eta_4 = \frac{1}{2}\sqrt{\left(\delta M_{xx}\right)^2 + \left(\delta M_{yy}\right)^2}\ . \tag{A.2b}$$

Errors of invariants I_1- I_7 and Q:

$$\delta I_k = \sum_{i=1}^{4}\left(\left(\frac{\partial I_k}{\partial \xi_i}\right)^2 \left(\delta\xi_i\right)^2 + \left(\frac{\partial I_k}{\partial \eta_i}\right)^2 \left(\delta\eta_i\right)^2\right)^{1/2}\ , \tag{A.3}$$

then,

$$\delta I_1 = \frac{1}{I_1}\sqrt{\xi_1^2\delta\xi_1^2 + \xi_4^2\delta\xi_4^2}\ , \tag{A.3}$$

$$\delta I_2 = \frac{1}{I_2}\sqrt{\eta_1^2\delta\eta_1^2 + \eta_4^2\delta\eta_4^2}\ , \tag{A.4}$$

$$\delta I_3 = \frac{1}{I_1^2 I_3}\sqrt{\xi_2^2\delta\xi_2^2 + \xi_3^2\delta\xi_3^2} + \frac{I_3}{I_1^2}\sqrt{\xi_1^2\delta\xi_1^2 + \xi_4^2\delta\xi_4^2}\ , \tag{A.5}$$

$$\delta I_4 = \frac{1}{I_2^2 I_4}\sqrt{\eta_2^2\delta\eta_2^2 + \eta_3^2\delta\eta_3^2} + \frac{I_4}{I_2^2}\sqrt{\eta_1^2\delta\eta_1^2 + \eta_4^2\delta\eta_4^2}\ , \tag{A.6}$$

$$\delta I_5 = \delta s_{41} = \frac{1}{I_1 I_2}\sqrt{\left(\eta_4 - I_5\xi_1\frac{I_2}{I_1}\right)^2\delta\xi_1^2 + \left(\eta_1 - I_5\xi_4\frac{I_2}{I_1}\right)^2\delta\xi_4^2 + \left(\xi_4 - I_5\eta_1\frac{I_1}{I_2}\right)^2\delta\eta_1^2 + \left(\xi_1 - I_5\eta_4\frac{I_1}{I_2}\right)^2\delta\eta_4^2}\ , \tag{A.7}$$

$$\delta d_{ij} = \frac{1}{I_1 I_2}\sqrt{\left(\eta_j - d_{ij}\xi_i\frac{I_2}{I_1}\right)^2\delta\xi_i^2 + \left(-\eta_i - d_{ij}\xi_j\frac{I_2}{I_1}\right)^2\delta\xi_j^2 + \left(-\xi_j - d_{ij}\eta_i\frac{I_1}{I_2}\right)^2\delta\eta_i^2 + \left(\xi_i - d_{ij}\eta_j\frac{I_1}{I_2}\right)^2\delta\eta_j^2}\ , \tag{A.8}$$

$$\delta I_6 = \delta d_{41} = \frac{1}{I_1 I_2}\sqrt{\left(\eta_1 - I_6\xi_4\frac{I_2}{I_1}\right)^2\delta\xi_4^2 + \left(-\eta_4 - I_6\xi_1\frac{I_2}{I_1}\right)^2\delta\xi_1^2 + \left(-\xi_1 - I_6\eta_4\frac{I_1}{I_2}\right)^2\delta\eta_4^2 + \left(\xi_4 - I_{41}\eta_1\frac{I_1}{I_2}\right)^2\delta\eta_1^2}\ , \tag{A.9}$$

$$\delta Q=\sqrt{\sum_{k=1}^{4}\left[\left(\sum_{\substack{ij=12,\\13,24,34}}\frac{\partial Q}{\partial d_{ij}}\frac{\partial d_{ij}}{\partial \xi_k}\right)^2\delta\xi_k^2+\left(\sum_{\substack{ij=12,\\13,24,34}}\frac{\partial Q}{\partial d_{ij}}\frac{\partial d_{ij}}{\partial \eta_k}\right)^2\delta\eta_k^2\right]}\,, \tag{A.10}$$

and

$$\delta I_7=\sqrt{\sum_{k=1}^{4}\left[\left(\frac{\partial I_7}{\partial Q}\sum_{\substack{ij=12,\\13,24,34}}\frac{\partial Q}{\partial d_{ij}}\frac{\partial d_{ij}}{\partial \xi_k}+\frac{\partial I_7}{\partial d_{41}}\frac{\partial d_{41}}{\partial \xi_k}+\frac{\partial I_7}{\partial d_{23}}\frac{\partial d_{23}}{\partial \xi_k}\right)^2\delta\xi_k^2+\left(\frac{\partial I_7}{\partial Q}\sum_{\substack{ij=12,\\13,24,34}}\frac{\partial Q}{\partial d_{ij}}\frac{\partial d_{ij}}{\partial \eta_k}+\frac{\partial I_7}{\partial d_{41}}\frac{\partial d_{41}}{\partial \eta_k}+\frac{\partial I_7}{\partial d_{23}}\frac{\partial d_{23}}{\partial \eta_k}\right)^2\delta\eta_k^2\right]}\,, \tag{A.11}$$

with:

$$\frac{\partial Q}{\partial d_{12}}=\frac{1}{Q}\left(d_{12}-d_{34}\right)\text{ and }\frac{\partial Q}{\partial d_{34}}=-\frac{1}{Q}\left(d_{12}-d_{34}\right), \tag{A.12}$$

$$\frac{\partial Q}{\partial d_{13}}=\frac{\partial Q}{\partial d_{24}}=\frac{1}{Q}\left(d_{13}+d_{24}\right), \tag{A.13}$$

$$\frac{\partial d_{ij}}{\partial \xi_k}=\frac{1}{I_1 I_2}\left\{\begin{matrix}\eta_j\,,k=i\\ -\eta_i\,,k=j\\ 0\qquad,k\neq i\neq j\end{matrix}\right\}-d_{ij}\frac{1}{I_1}\left\{\begin{matrix}\xi_k/I_1\,,k=1,4\\ 0\qquad,k=2,3\end{matrix}\right\}, \tag{A.14}$$

$$\frac{\partial d_{ij}}{\partial \eta_k}=\frac{1}{I_1 I_2}\left\{\begin{matrix}-\xi_j\,,k=i\\ \xi_i\,,k=j\\ 0\qquad,k\neq i\neq j\end{matrix}\right\}-d_{ij}\frac{1}{I_2}\left\{\begin{matrix}\eta_k/I_2\,,k=1,4\\ 0\qquad,k=2,3\end{matrix}\right\}, \tag{A.15}$$

$$\frac{\partial I_7}{\partial Q}=-\frac{1}{Q^2}\left(d_{41}-d_{23}\right), \tag{A.16}$$

$$\frac{\partial I_7}{\partial d_{41}}=\frac{1}{Q}\text{ and }\frac{\partial I_7}{\partial d_{23}}=\frac{-1}{Q}. \tag{A.17}$$

Strike angles, θ_1 and θ_2, θ_D and θ_3 and their errors, using classical error propagation as well:

$$\theta_1 = \frac{1}{2}\arctan\left(\frac{-\xi_3}{\xi_2}\right) \tag{A.18}$$

$$\delta\theta_1 = \frac{1}{2}\frac{1}{1+\left(-\xi_3/\xi_2\right)^2}\sqrt{\left(\frac{\xi_3}{\xi_2^2}\right)^2\delta\xi_2^2 + \left(\frac{-1}{\xi_2}\right)^2\delta\xi_3^2}\ , \tag{A.19}$$

$$\theta_2 = \frac{1}{2}\arctan\left(\frac{-\eta_3}{\eta_2}\right), \tag{A.20}$$

$$\delta\theta_2 = \frac{1}{2}\frac{1}{1+\left(-\eta_3/\eta_2\right)^2}\sqrt{\left(\frac{\eta_3}{\eta_2^2}\right)^2\delta\eta_2^2 + \left(\frac{-1}{\eta_2}\right)^2\delta\eta_3^2}\ , \tag{A.21}$$

$$\theta_D = \frac{1}{2}\arctan\left(\frac{\xi_2}{\xi_3}\right)\ , \quad \text{(or using imaginary components } \eta_2 \text{ and } \eta_3\text{)} \tag{A.22}$$

$$\delta\theta_D = \frac{1}{2}\frac{1}{1+\left(\xi_3/\xi_2\right)^2}\sqrt{\left(\frac{1}{\xi_3}\right)^2\delta\xi_2^2 + \left(\frac{-\xi_2}{\xi_3^2}\right)^2\delta\xi_3^2}\ , \tag{A.23}$$

$$\theta_3 = \frac{1}{2}\arctan\left(\frac{d_{12}-d_{34}}{d_{13}+d_{24}}\right), \tag{A.24}$$

$$\delta\theta_3 = \frac{1}{2}\frac{1}{1+\left(\dfrac{d_{12}-d_{34}}{d_{13}+d_{24}}\right)^2}\sqrt{\left(\frac{1}{d_{13}+d_{24}}\right)^2\cdot\left(\delta d_{12}^2+\delta d_{34}^2\right)+\left(\frac{-(d_{12}-d_{34})}{\left(d_{13}+d_{24}\right)^2}\right)^2\cdot\left(\delta d_{13}^2+\delta d_{24}^2\right)}\ , \tag{A.25}$$

where errors of d_{ij} are those of equation A.8.

The errors of distortion parameters ϕ_1 and ϕ_2 are not shown, given their complex dependence on all the magnetotelluric components and the strike angle (e.g. $\phi_1=f(M_{xx}, M_{xy}, M_{yx}, M_{yy}, \theta_3)$), and the fact that these errors are better resolved using random gaussian noise generation.

Appendix B: The COPROD2 Dataset: Geological Setting and Responses from Site 85_314

The COPROD2 is an MT dataset collected along a 400 km EW profile in southern Saskatchewan and Manitoba (Canada), at 49°N, and from 106°W to 100°W, crossing the thick Paleozoic sediments of the Willingston basin. Within the basement beneath the sediments lies one of the world's longest and most enigmatic crustal conductivity features: the North American Central Plains (NACP) conductivity anomaly. At the eastern extreme of the profile there is a second basement anomaly (TOBE) interpreted as being associated with the Thompson Nickel Belt at the Superior-Churchill boundary (Figure B.1).

Data have a wide bandwidth (2.6ms to 1820s) and are of high quality (impedance errors typically <2%) (Jones, 1993). These data were made available to the MT community and are commonly used to test and compare 2D inversion codes, as in general these have a 2D behaviour. Presently, these data can be downloaded from the MTNET web page (http://www.mtnet.info).

Site 85_314, which has been used through this thesis to test different methodologies, is located in the central part of the COPROD2 profile. Figures B.2 and B.3 display the MT tensor components, apparent resistivities and phases, with the corresponding error bars, computed at this site.

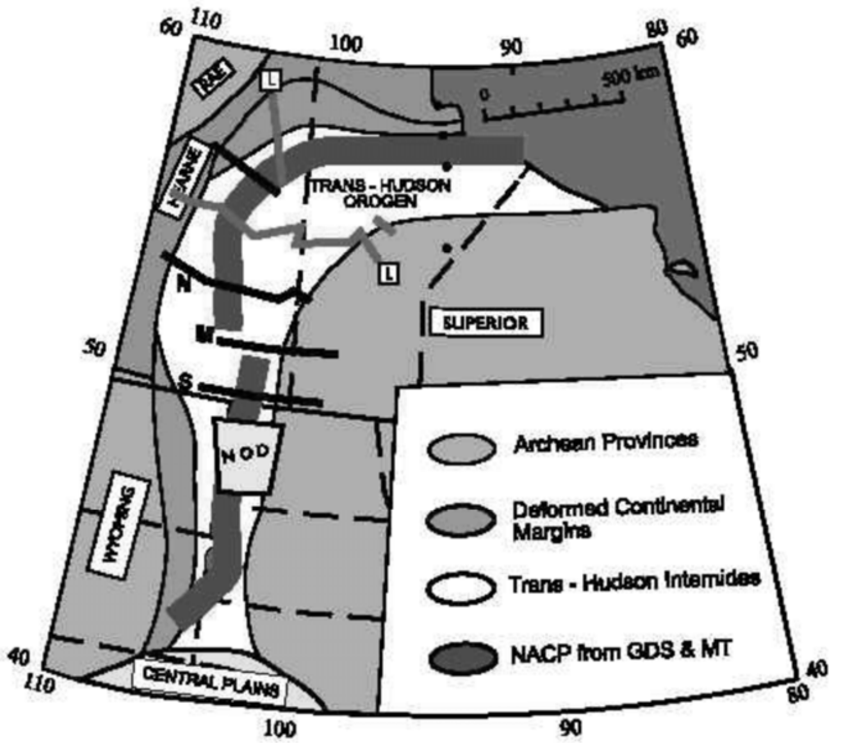

Figure B.1: The North American Central Plains (NACP) anomaly within the Trans-Hudson orogen. Also shown, the locations of the MT surveys. S: Coprod2 profile. (From Jones *et al.*, 2005).

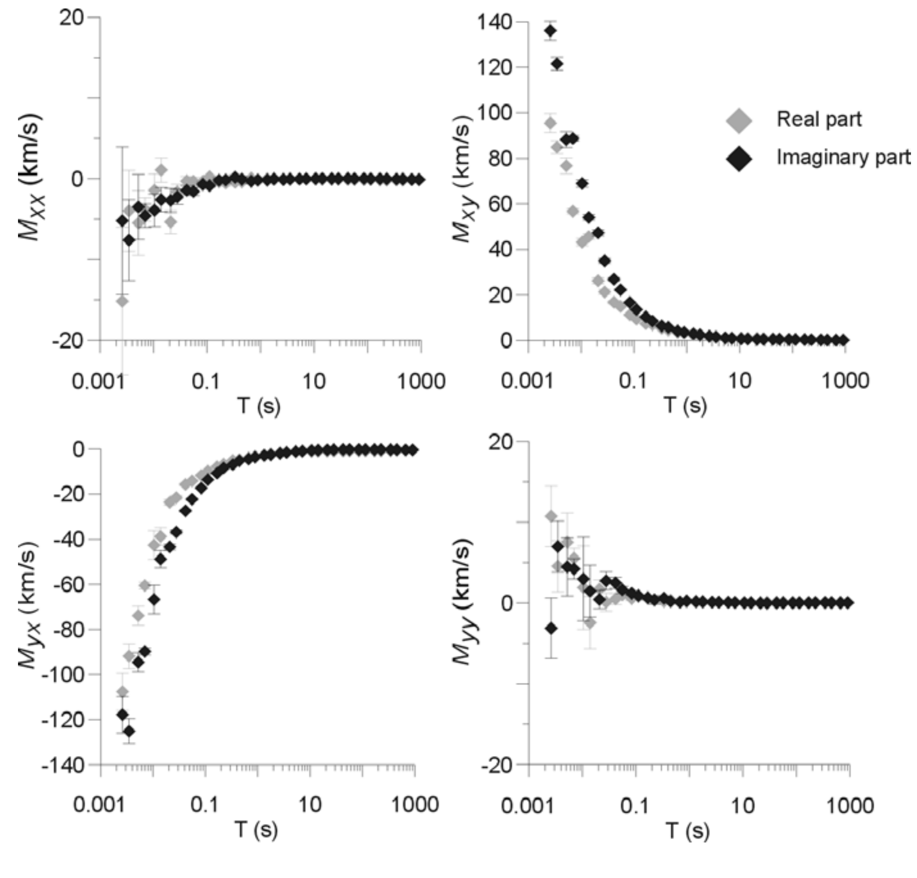

Figure B.2: Magnetotelluric tensor components of site 85_314 from the COPROD2 dataset.

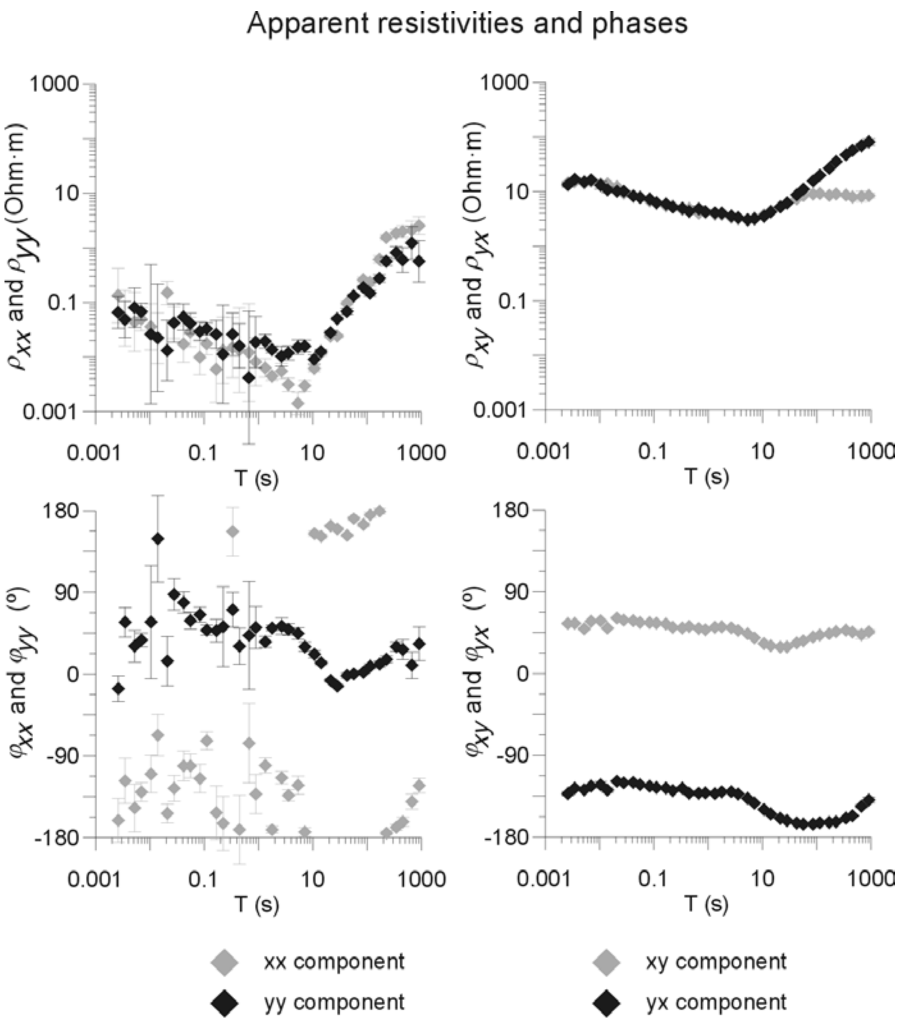

Figure B.3: Apparent resistivity and phase computed from MT tensor components of the COPROD2 site 85_314

Appendix C: The BC87 dataset: Geological Setting and Main Features of the MT Responses

The BC87 dataset was acquired in southeastern British Columbia as part of the LITHOPROBE project. This dataset is commonly used too to test and compare new methods in analysis and interpretation of MT data (Jones *et al.*, 1993), and especially to show the limitations of 2D interpretation of MT data (Chave and Jones, 1997). It consists of 27 sites along an approximate E-W profile (Figure C.1).

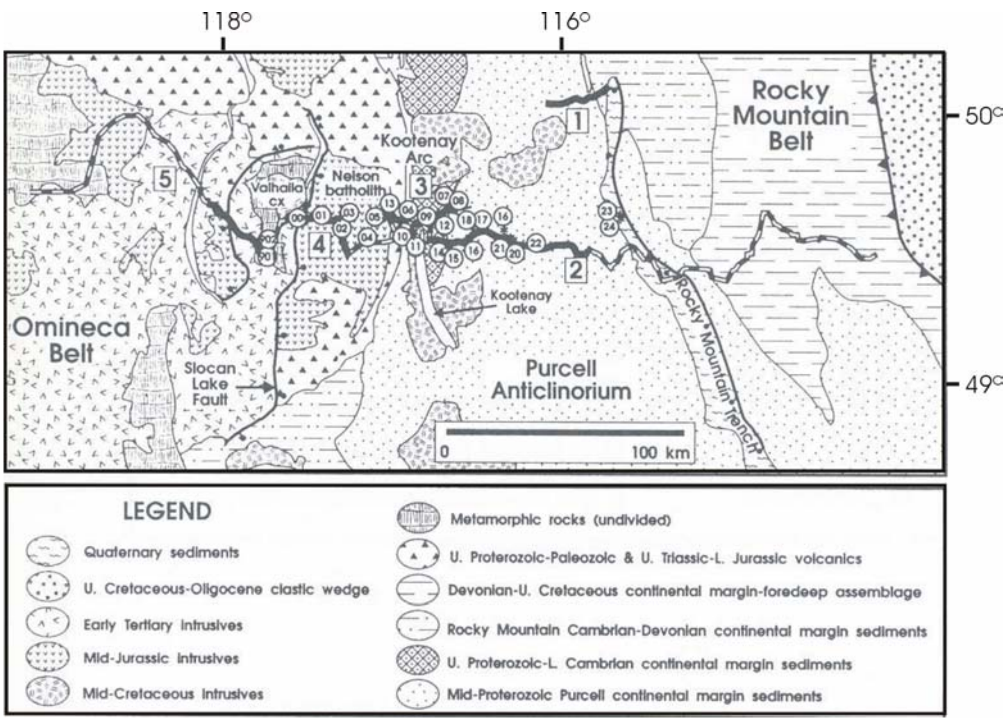

Figure C.1: BC87 geological setting and location of MT sites. Site 4 is located above Nelson Batholith.

Data display complex 3D effects, due both to local effects and the presence of the Nelson Batholith body (western part of profile). Site 4 is located above this body. The responses at this site (magnetotelluric tensor components and apparent resistivities and phases) are shown in Figures C.1 and C.2. Presently, these data are available from the MTNET web page.

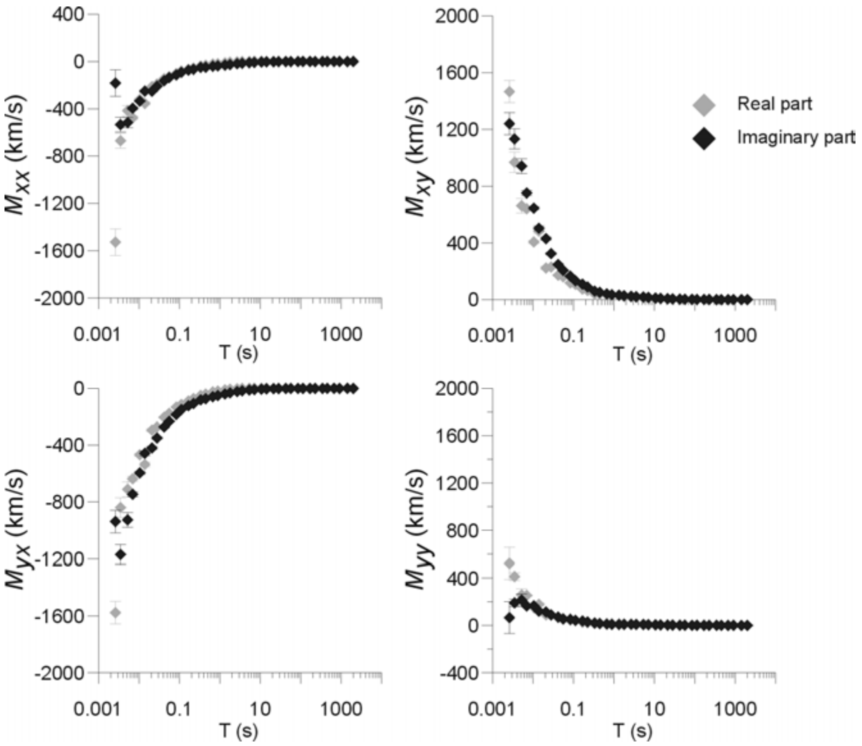

Figure C.2: Magnetotelluric tensor components of site 4 from the BC87 dataset.

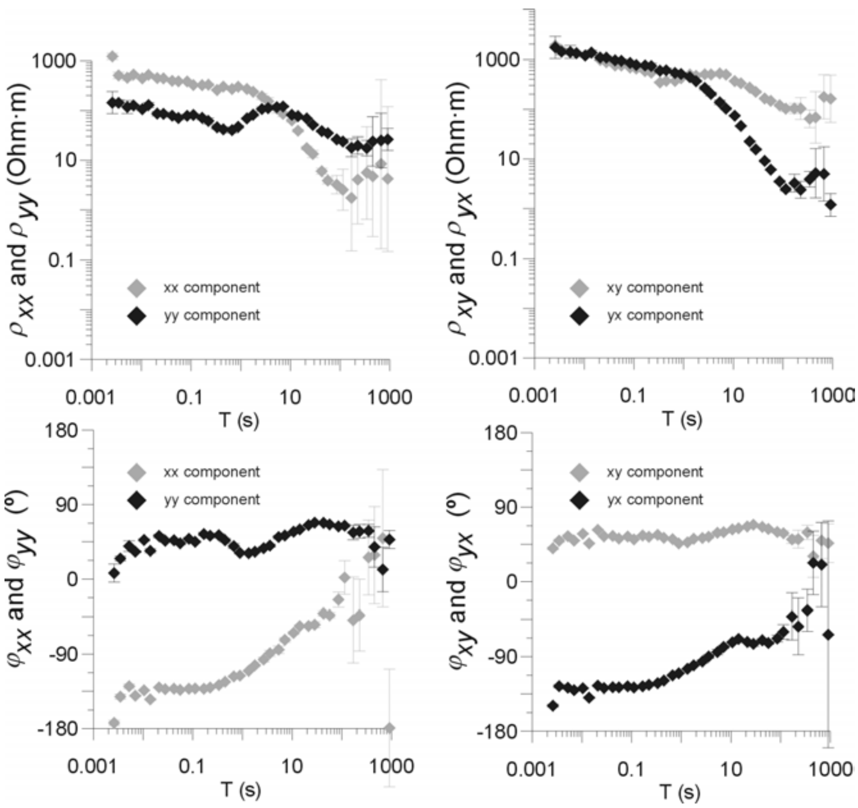

Figure C.3: Apparet resistivity and phases computed from MT tensor components of site 4 from the BC87 dataset.

Appendix D: Betics Dataset Locations and Responses

Site id	Zone	Geographical coordinates		Alt. (m)	Tipper?	# or estimated periods and range	Data quality	% of periods used in modelling
		Latitude	Longitude					
b01	Guadix-Baza Basin - Sª de Baza	+37:26:31	-2:52:07	1240	yes	40 4ms-4000s	GOOD	83
b02	Guadix-Baza Basin - Sª de Baza	+37:28:35	-2:54:13	1050		39 4ms-4000s	POOR	82
b03	Subbetic - Guadix-Baza Basin	+37:37:37	-3:02:14	620	yes	38 4ms-2000s	GOOD	92
b04	Subbetic - Guadix-Baza Basin	+37:37:43	-3:07:57	840				
b05	Subbetic - Guadalquivir Basin	+37:50:09	-3:09:49	520	yes	40 4ms-4000s	GOOD	90
b06	Subbetic - Guadalquivir Basin	+37:52:38	-3:12:16	420		34 4ms-500s	MEDIUM	94
b07	Iberian Massif	+38:08:37	-3:23:20	420	yes	40 4ms-4000s	MEDIUM	75
b08	Iberian Massif - Guadalquivir Basin	+38:05:58	-3:21:25	500		34 4ms-500s	MEDIUM	44
b09	Iberian Massif	+38:13:34	-3:14:03	650		39 4ms-4000s	VERY POOR	0
b11	Iberian Massif	+38:16:15	-3:21:56	550	yes	34 4ms-500s	GOOD	91
b13	Iberian Massif	+38:26:25	-3:43:39	850		34 4ms-500s	GOOD	85

b14	Iberian Massif	+38:30:16	-3:57:06	650		32 4ms-500s	MEDIUM	81
b15	Sª de la Contraviesa (Alpujárride)	+36:54:37	-3:07:24	1160		41 4ms-4000s	GOOD	85
b16	Sª Nevada	+37:03:32	-3:03:10	2160	yes			
b17	Sª de los Filabres	+37:14:04	-2:43:46	1920	yes	34 4ms-500s	VERY GOOD	97
b18	Sª de Baza (nevado	+37:20:44	-2:51:40	1740	yes	40 4ms-4000s	GOOD	100
b19	Sª de las Estancias (Alpujárride)	+37:30:54	-2:20:17	1360	yes	40 4ms-4000s	GOOD	98
b20	Sª de María (Prebetic)	+37:38:51	-2:20:25	1340	yes	32 4ms-300s	MEDIUM	81
b21	Guadix-Baza Basin	+37:45:39	-2:18:27	1100	yes	32 4ms-200s	GOOD	88
b22	Sª de la Sagra	+37:55:56	-2:31:19	1450				
b23	Guadix-Baza Basin	+37:42:59	-2:36:10	860	yes	40 4ms-4000s	GOOD	95
b24	Sª de Segura (Prebetic)	+38:00:34	-2:42:01	1660	yes	40 4ms-4000s	GOOD	98
b26	Sª de Cazorla (Prebetic)	+38:07:05	-2:55:53	1340	yes	40 4ms-4000s	VERY GOOD	93
b27	Guadix-Baza Basin	+37:31:05	-3:23:45	1200	yes	40 4ms-4000s	GOOD	93
b28	Sª Mágina (Subbetic)	+37:44:52	-3:25:52	1640				
b29	Sª de los Filabres	+37:16:31	-2:18:35	1080	yes	32 4ms-300s	MEDIUM	72
b30	Sª de los Filabres	+37:08:56	-2:15:06	700	yes	40 4ms-4000s	VERY GOOD	95
b31	Sª de Alhamilla (Nevado-Filábride)	+36:59:50	-2:14:41	920	yes	29 4ms-300s	GOOD	97
b32	Tabernas Basin - Sª de los Filabres	+37:04:02	-2:25:24	420	yes	32 4ms-300s	MEDIUM	81
b33	Sª de Gádor (Alpujárride)	+37:03:36	-2:15:11	1050		40 4ms-4000s	MEDIUM	80
b34	Sª de los Filabres	+37:04:54	-2:47:53	2000				
b35	Sª de los Filabres	+37:05:42	-2:44:10	1080	yes	35 4ms-500s	GOOD	80
b36	Guadix-Baza - Almanzora Basin (North of Sª de los Filabres)	+37:18:45	-2:35:43	1320		41 4ms-4000s	MEDIUM	88
b37	Sª de las Estancias (Alpujárride)	+37:27:12	-2:25:42	1220	yes	40 4ms-4000s	MEDIUM	93
b38	Sª Arana (Alpujárride)	+37:21:15	-3:25:45	1050	yes	40 4ms-4000s	POOR	73
b39	Sª Nevada	+37:13:10	-3:13:30	1150	yes	41 4ms-4000s	MEDIUM	95
b40	Sª Mágina (Subbetic)	+37:53:36	-3:28:48	440	yes	41 4ms-4000s	MEDIUM	95

b41	Sª Mágina (Subbetic)	+37:36:17	-3:26:12	1100		32 4ms-4000s	GOOD	66
b51	Guadix-Baza Basin	+37:22:30	-2:42:47	1150	yes	51 1ms-4000s	GOOD	82
b52	Sª de Baza (Alpujárride)	+37:17:04	-2:46:48	1950		48 1ms-1000s	MEDIUM	92
b53	Guadix-Baza Basin	+37:28:15	-2:34:51	1100	yes	51 1ms-4000s	GOOD	76
b54	Sª de Baza (Alpujárride)	+37:17:41	-2:55:38	1700	yes	49 1ms-4000s	MEDIUM	90
b55	Sª Nevada	+37:03:27	-3:03:17	2230	yes	39 1ms-100s	MEDIUM	77
b56	Sª de Gádor (Alpujárride)	+36:55:16	-2:54:01	1680	yes	50 1ms-2000s	MEDIUM	88
b57	Sª de los Filabres	+37:12:42	-2:36:39	2000	yes (LF1 and LF2)	50 1ms-2000s	MEDIUM	100
b58	Sª de los Filabres	+37:11:19	-2:22:15	900	yes	49 1ms-2000s	MEDIUM	90
b59	Tabernas Basin - Sª de los Filabres	+37:11:38	-2:08:53	650	yes	50 1ms-2000s	GOOD	90
b60	Almanzora Basin (East of Sª de los Filabres)	+37:25:24	-2:05:48	610	yes	48 1ms-1000s	MEDIUM	81

Table D.1: Betics MT dataset site information: Site identification, geographic and geologic location, geographical coordinates, altitude and whether tipper was recorded or not. Evaluated responses: # of periods estimated and period range used in the dimensionality analysis; data quality (see forthcoming text) and % of periods used in modelling. Grey: sites rejected due to the impossibility of doing adequate data processing (not enough long time series, highly contaminated segments or extremely low coherence values).

Sites	**Band names and sampling frequencies (or periods)**					
b01-b41		band1 (1kHz)		band2 (32Hz)	band3 (1s)	band4 (32s)
b51-b60	HF (40960 Hz)	LF1 (4096 Hz)	Free (512 Hz)	LF2 (64 Hz)	LF3 (2 Hz)	LF4 (T=16s, from LF3 resampling)

Table D.2: Band names and sampling frequencies of periods employed in data acquisition using Metronix MS-03 (sites b01 to b41) and Metronix MS-06 (sites b51 to b60) systems. Bands from both systems are aligned according to their sampling frequencies proximity.

A quality parameter of the data was evaluated based on the average coherence values and relative errors at each site:

$$Q_D = \frac{\overline{coh} + \left(1 - \overline{\varepsilon_M}\right)}{2}, \tag{D.1}$$

where $\overline{coh}$ is the average of bivariate coherences of one site,

$$\overline{coh} = \frac{\sum_{i=1}^{nfreq}\left(coh(E_x)_i + coh(E_y)_i\right)}{2 \cdot nfreq}, \qquad \text{(D.2)}$$

and $\overline{\varepsilon}$ is the average of the relative errors of all MT tensor components of one site:

$$\overline{\varepsilon} = \frac{\sum_{i=1}^{nfreq}\left(\varepsilon_{rel}(M_{xx}) + \varepsilon_{rel}(M_{xy}) + \varepsilon_{rel}(M_{yx}) + \varepsilon_{rel}(M_{yy})\right)}{4 \cdot nfreq}. \qquad \text{(D.3)}$$

The quality is then classified according to the criterion displayed in Table D.3, which was established from a comparison between Q_D values and a visual inspection of Betics dataset data.

Q_D>0.9	VERY GOOD
0.8<Q_D<0.9	GOOD
0.6<Q_D<0.8	MEDIUM
0.5<Q_D<0.6	POOR
Q_D<0.5	VERY POOR

Table D.3: Quality data criterion according to Q_D, which considers coherence values and data errors.

The following figures present all the magnetotelluric responses, resistivities, phases and tipper components, with their error bars, and induction arrows corresponding to the tipper real part, obtained at all sites. These are raw curves, referenced to NS-EW orientation axes. With the exception of the induction arrows, all estimated periods are displayed.

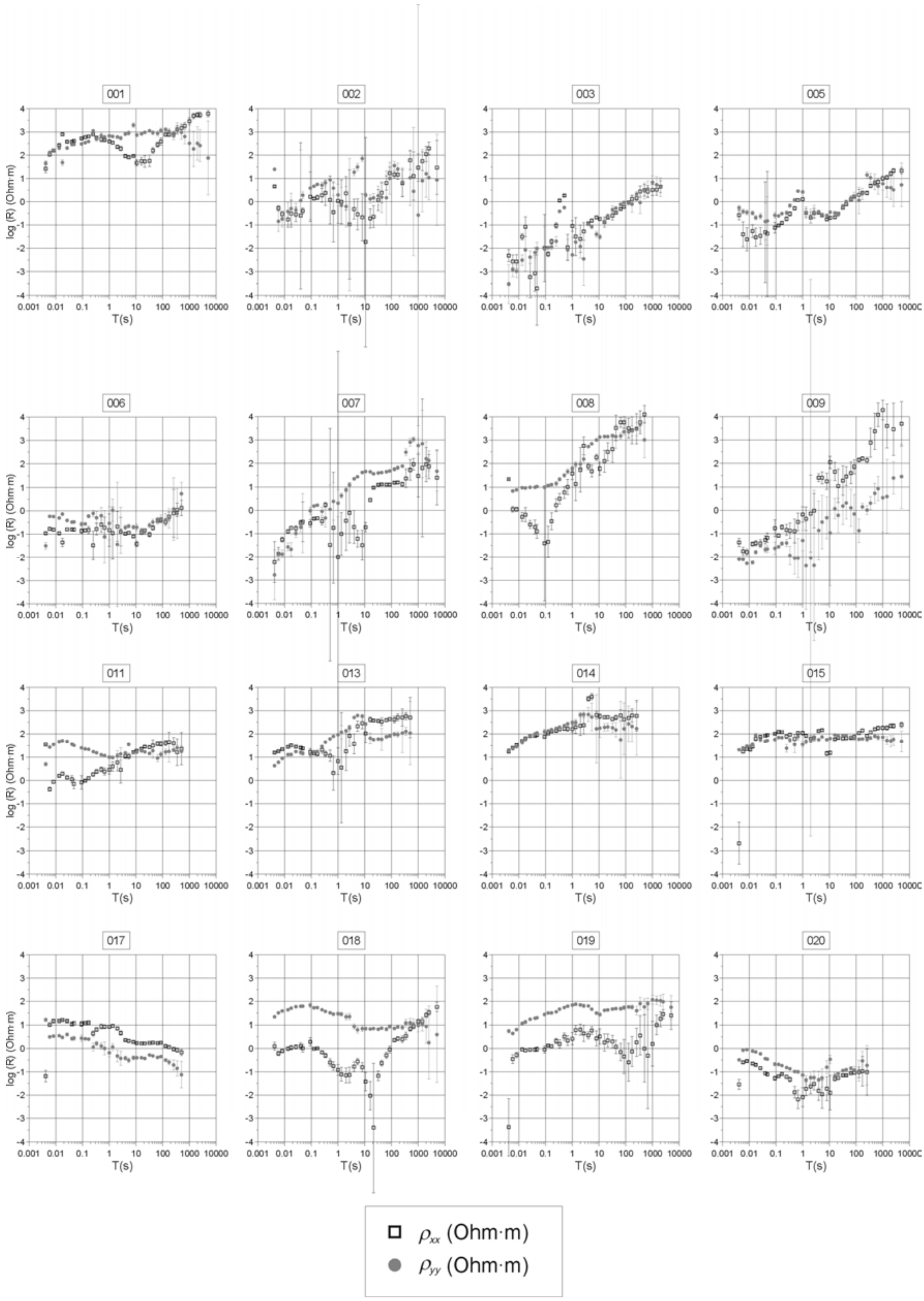

Figure D.1: Resistivity responses (ρ_{xx}, ρ_{xy}, ρ_{yx} and ρ_{yy}) with error bars for sites 001 to 020 from the Betics MT dataset.

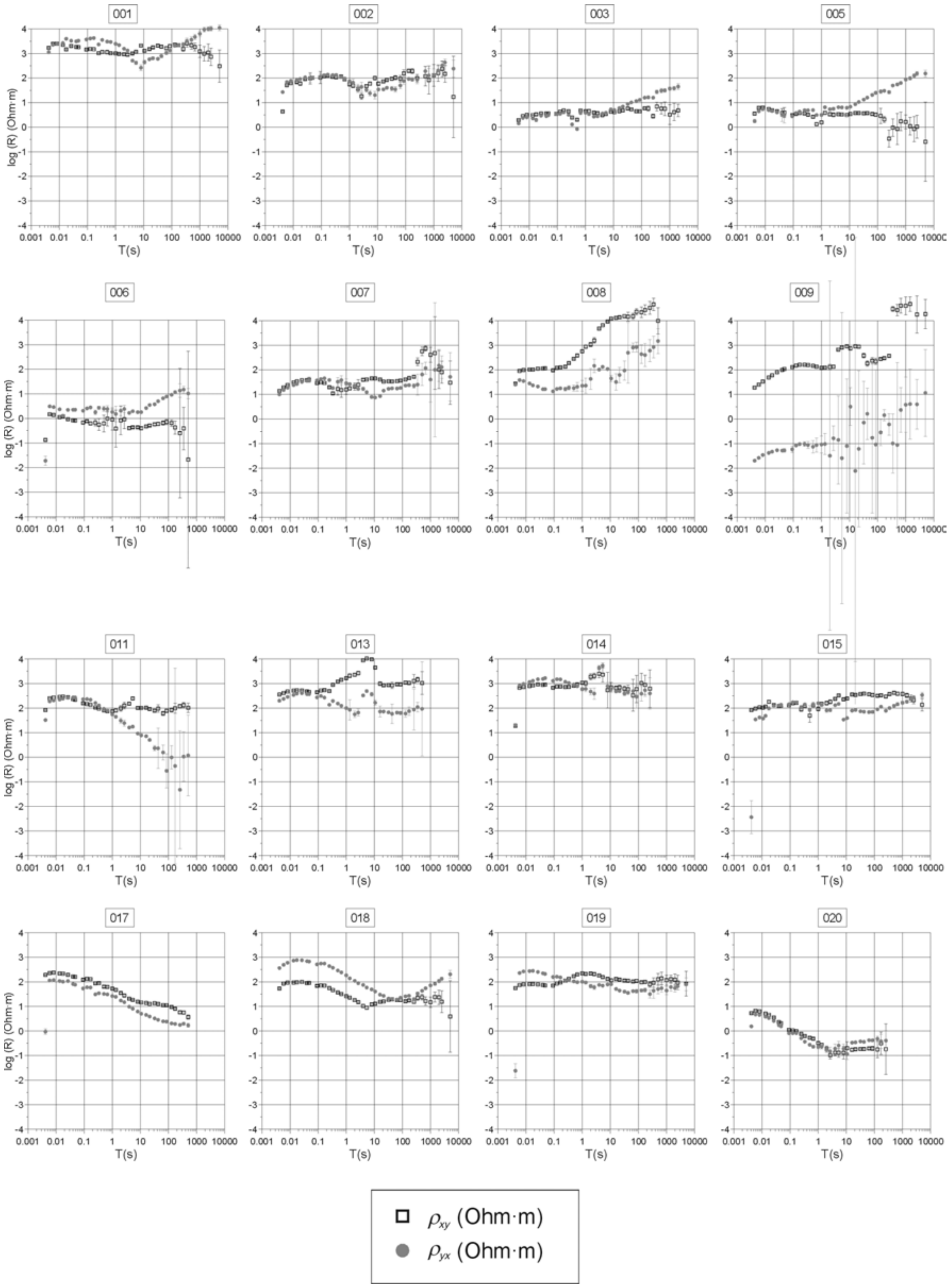

Figure D.1 (cont.)

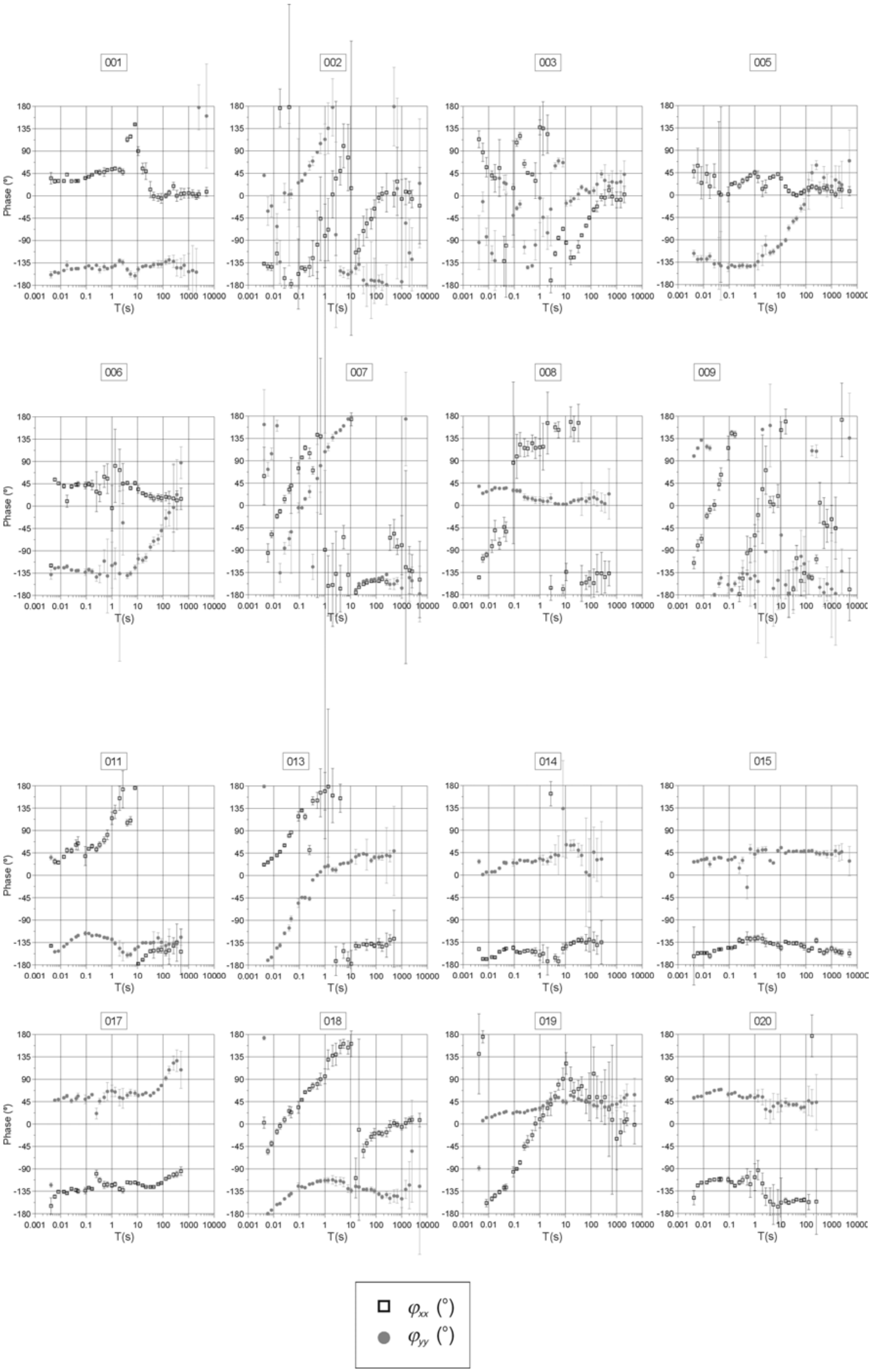

Figure D.2: Phase responses *(φ_{xx}, φ_{xy}, φ_{yx}* and *φ_{yy}*) with error bars for sites 001 to 020 from the Betics MT dataset.

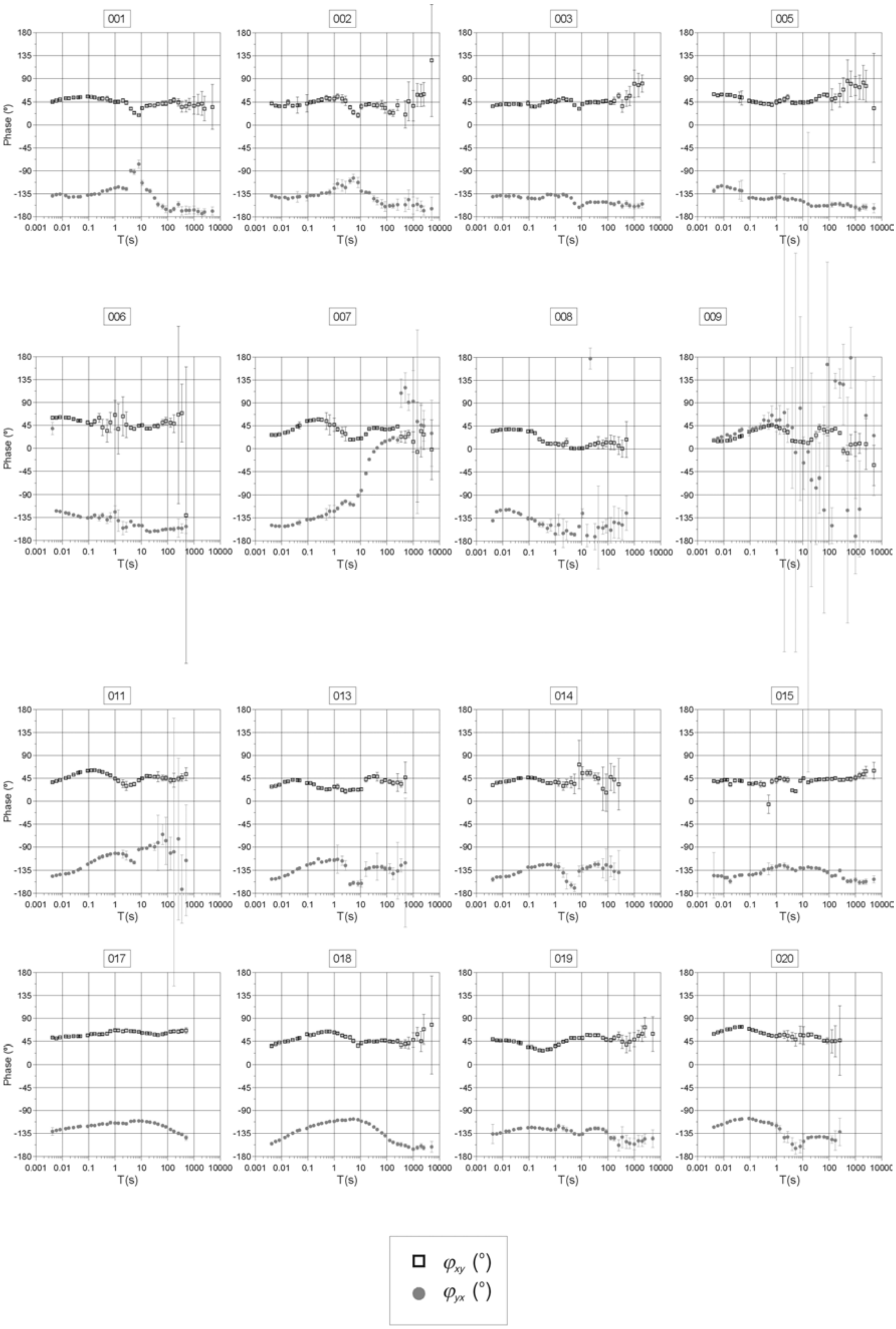

Figure D.2 (cont.)

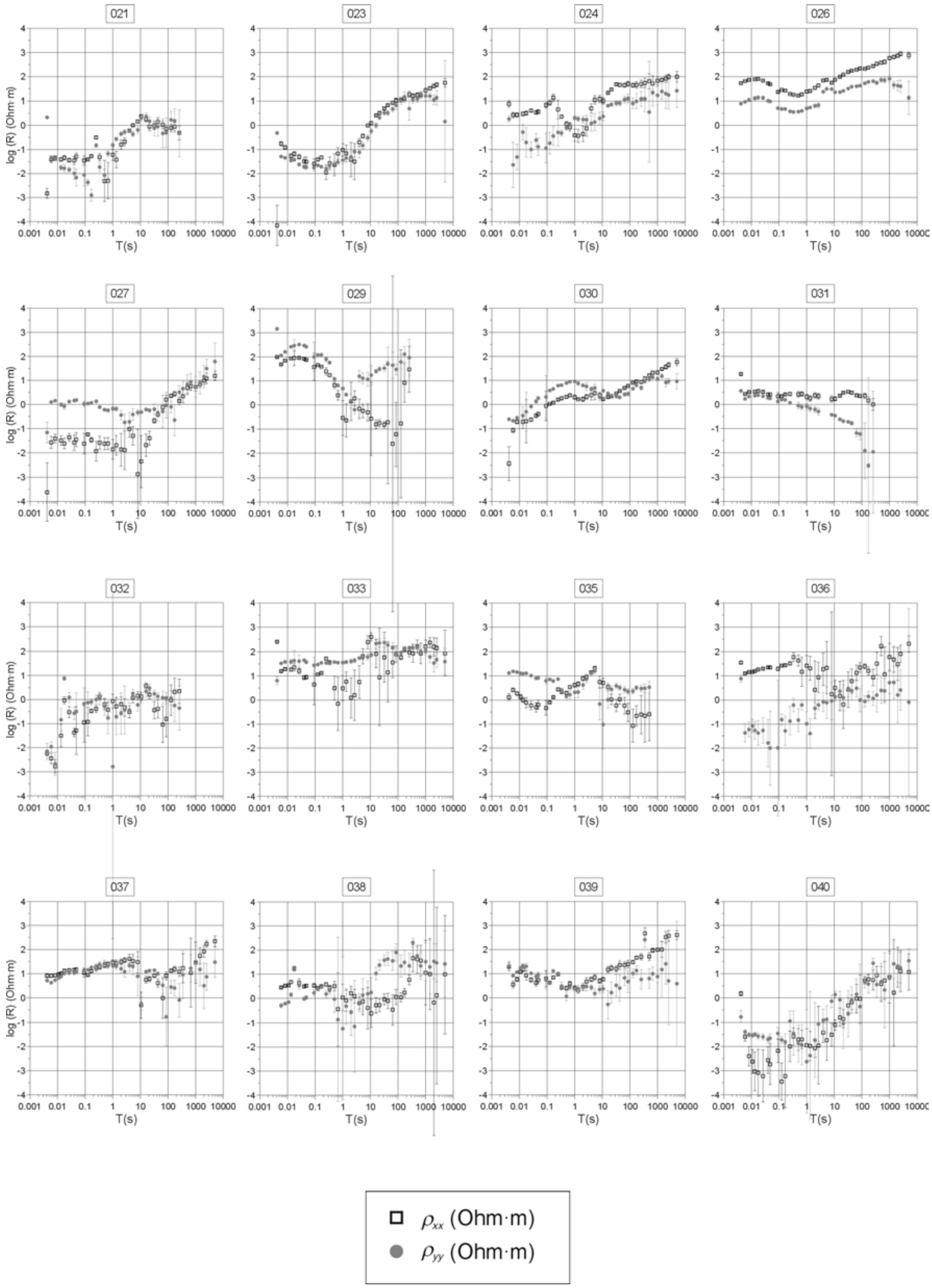

Figure D.3: Resistivity responses (ρ_{xx}, ρ_{xy}, ρ_{yx} and ρ_{yy}) with error bars for sites 021 to 040 from the Betics MT dataset.

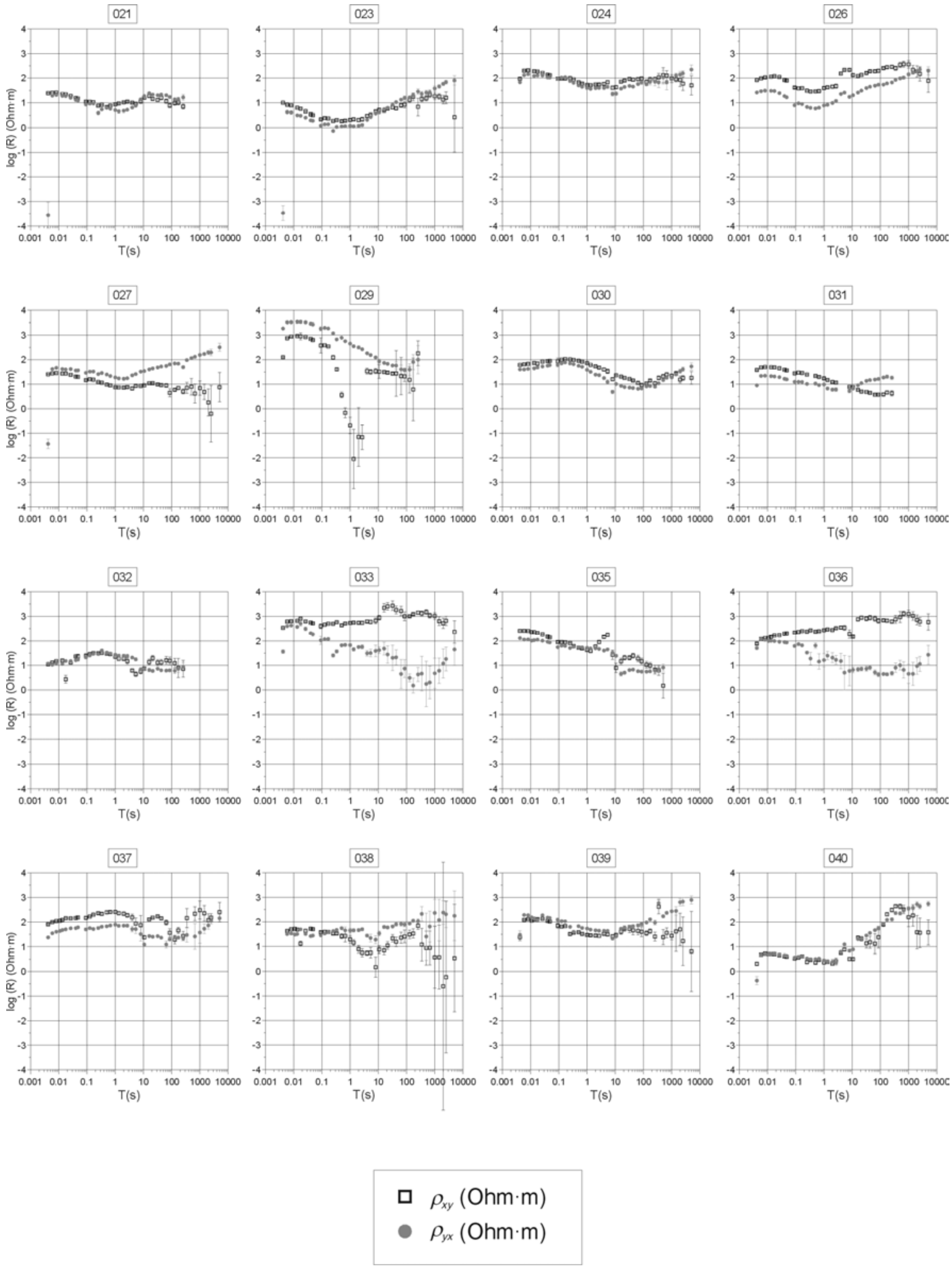

Figure D.3 (cont.)

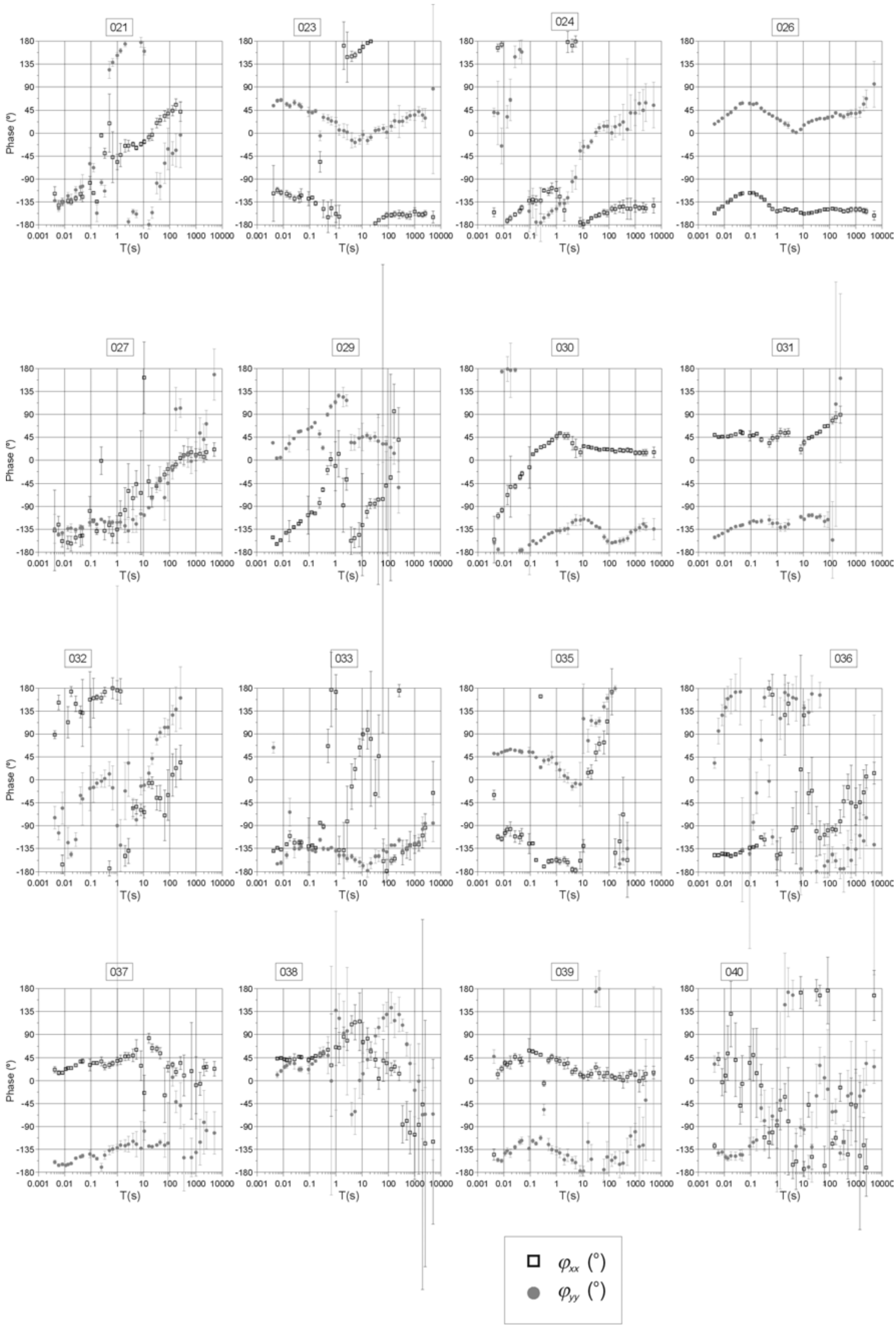

Figure D.4: Phase responses (φ_{xx}, φ_{xy}, φ_{yx} and φ_{yy}) with error bars for sites 021 to 040 from the Betics MT dataset.

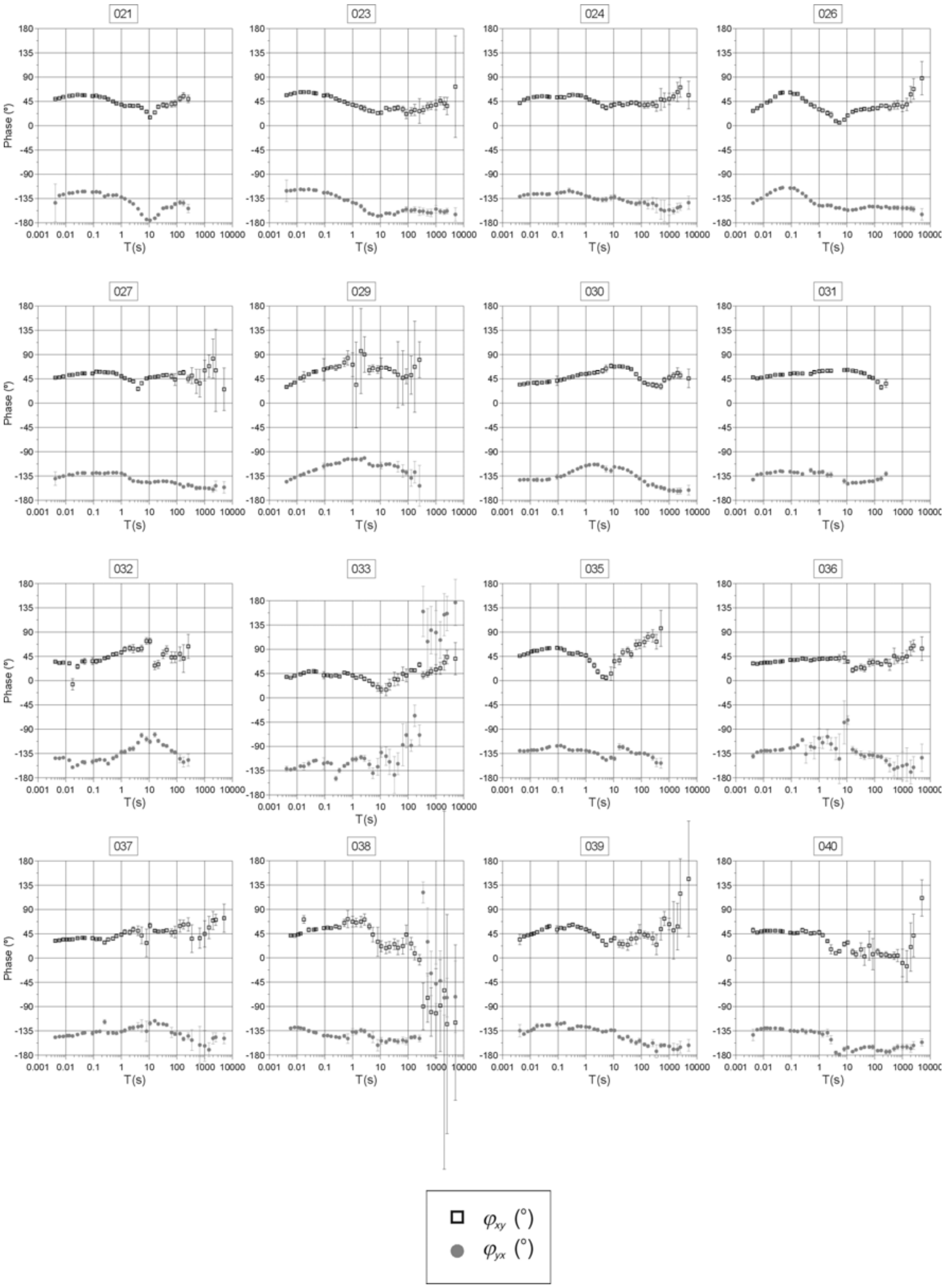

Figure D.4 (cont.)

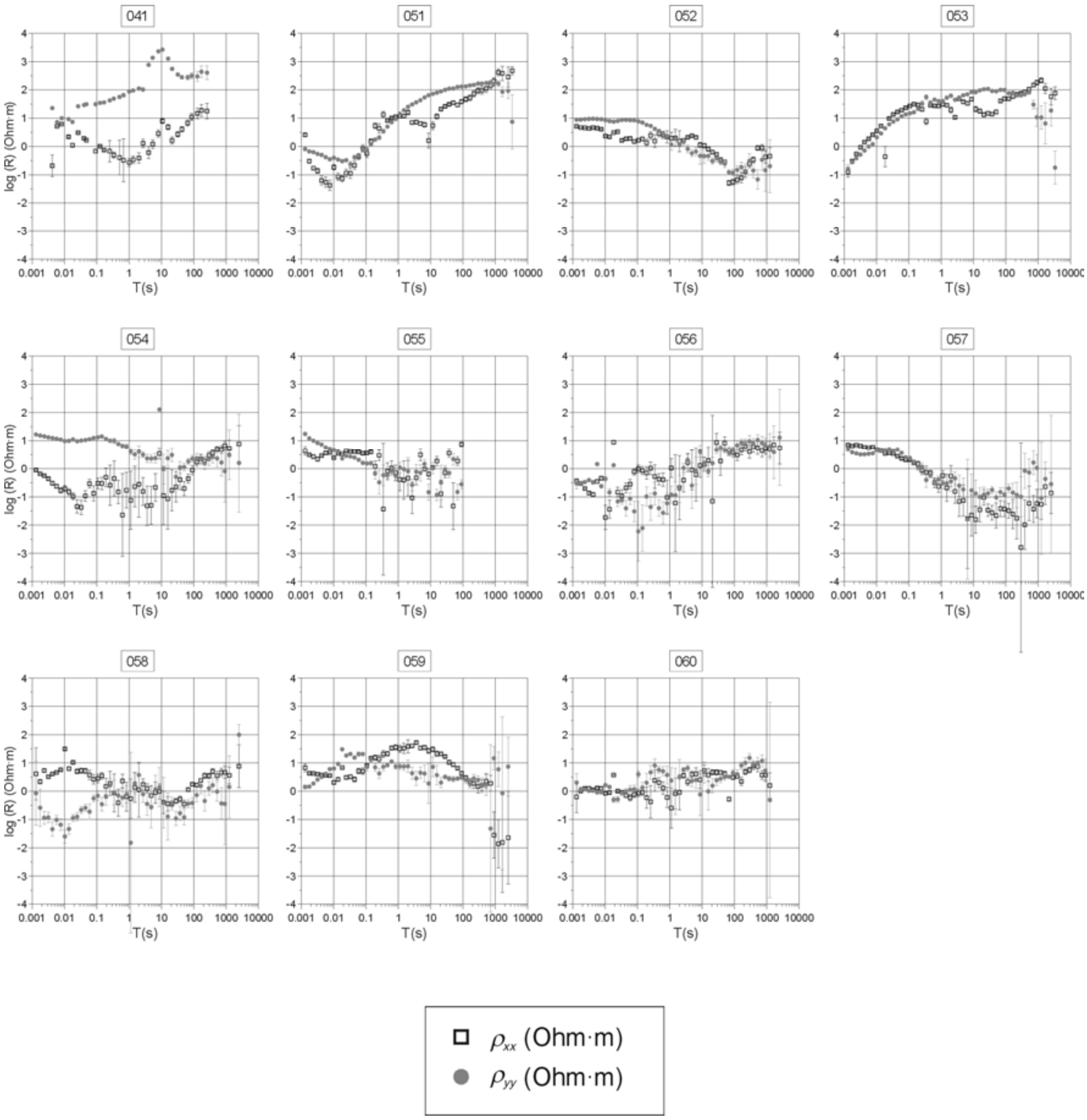

Figure D.5: Resistivity responses (ρ_{xx}, ρ_{xy}, ρ_{yx} and ρ_{yy}) with error bars for sites 041 to 060 from the Betics MT dataset.

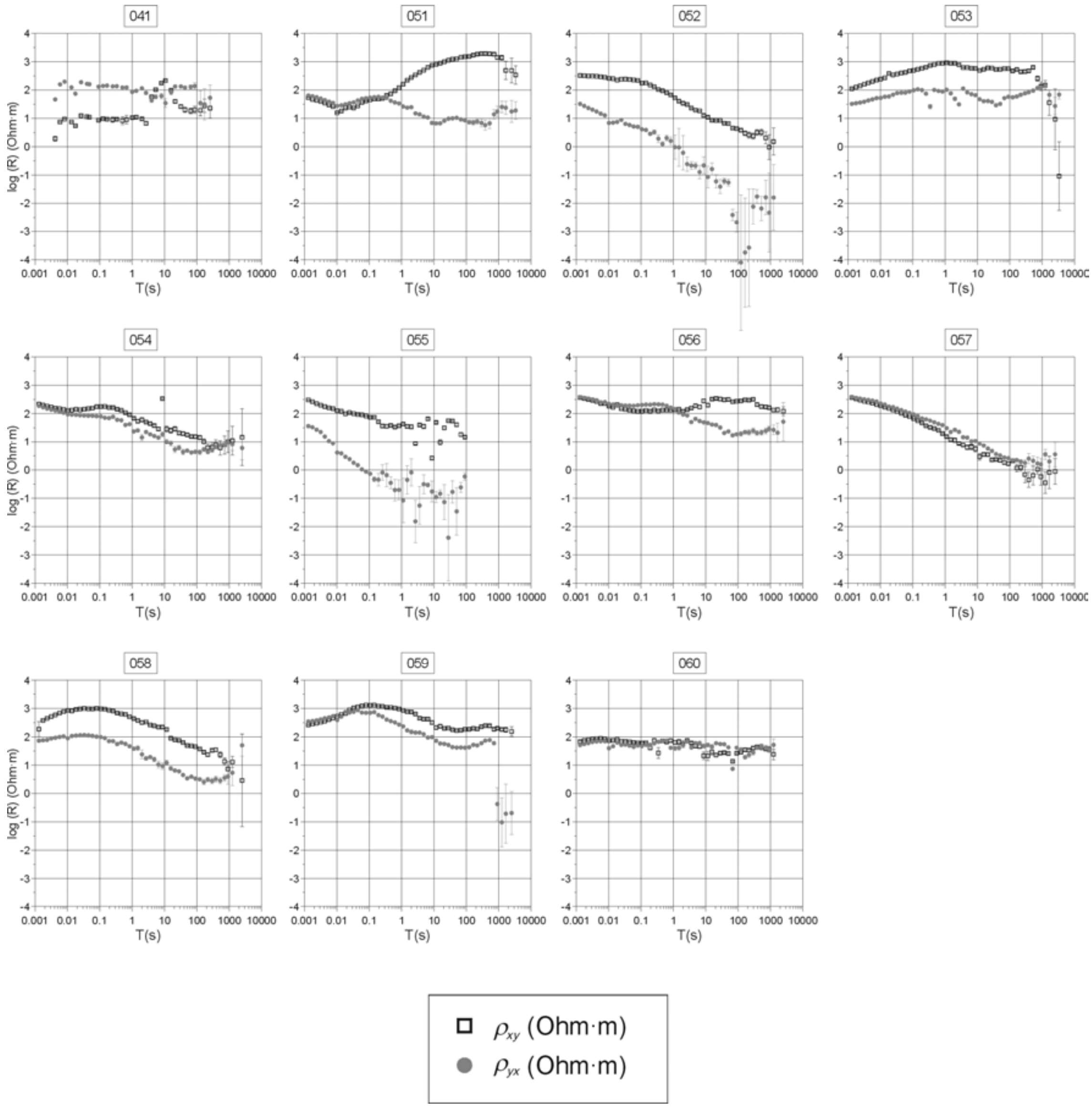

Figure D.5 (cont.)

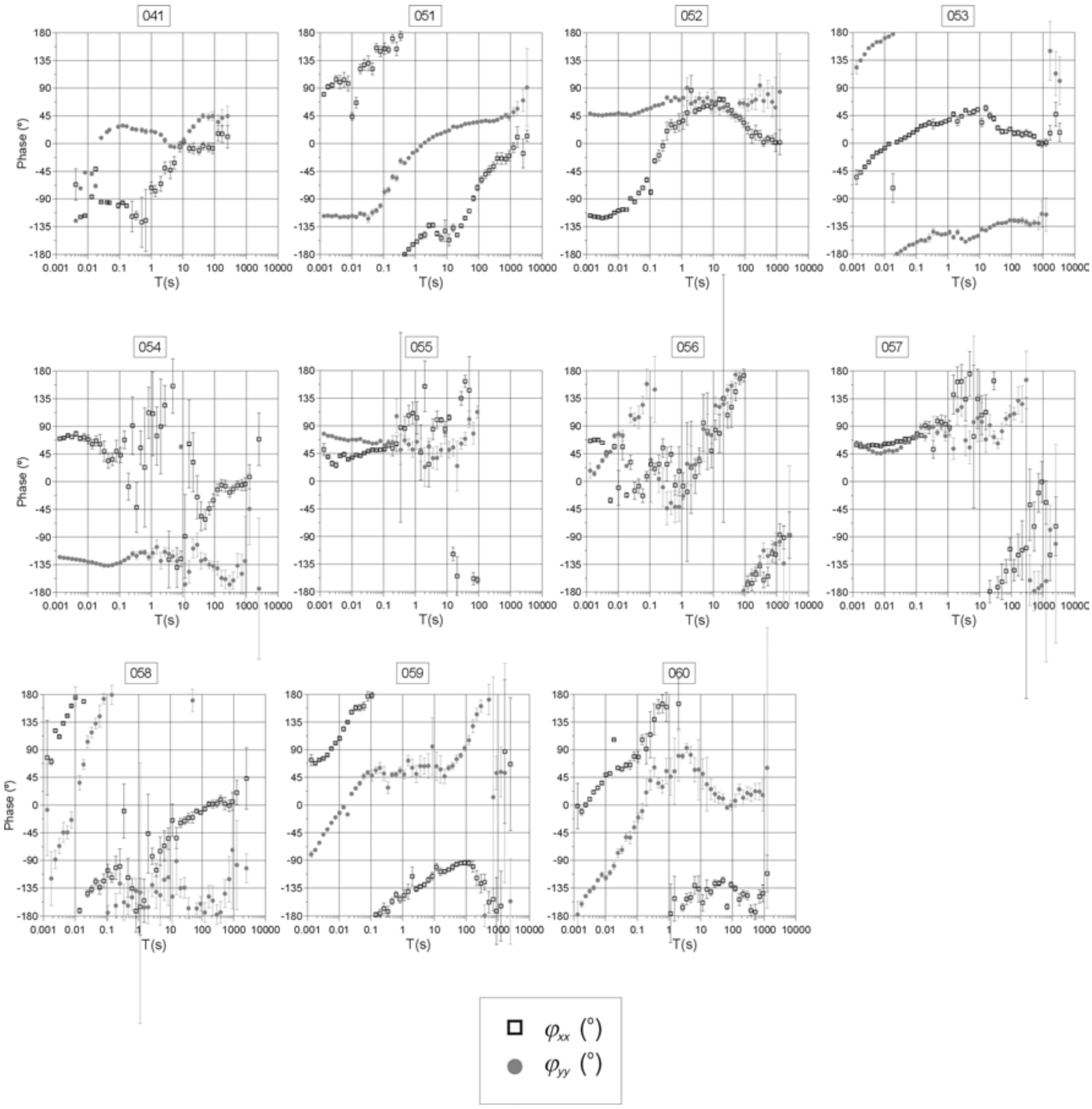

Figure D.6: Phase responses (φ_{xx}, φ_{xy}, φ_{yx} and φ_{yy}) with error bars for sites 041 to 060 from the Betics MT dataset.

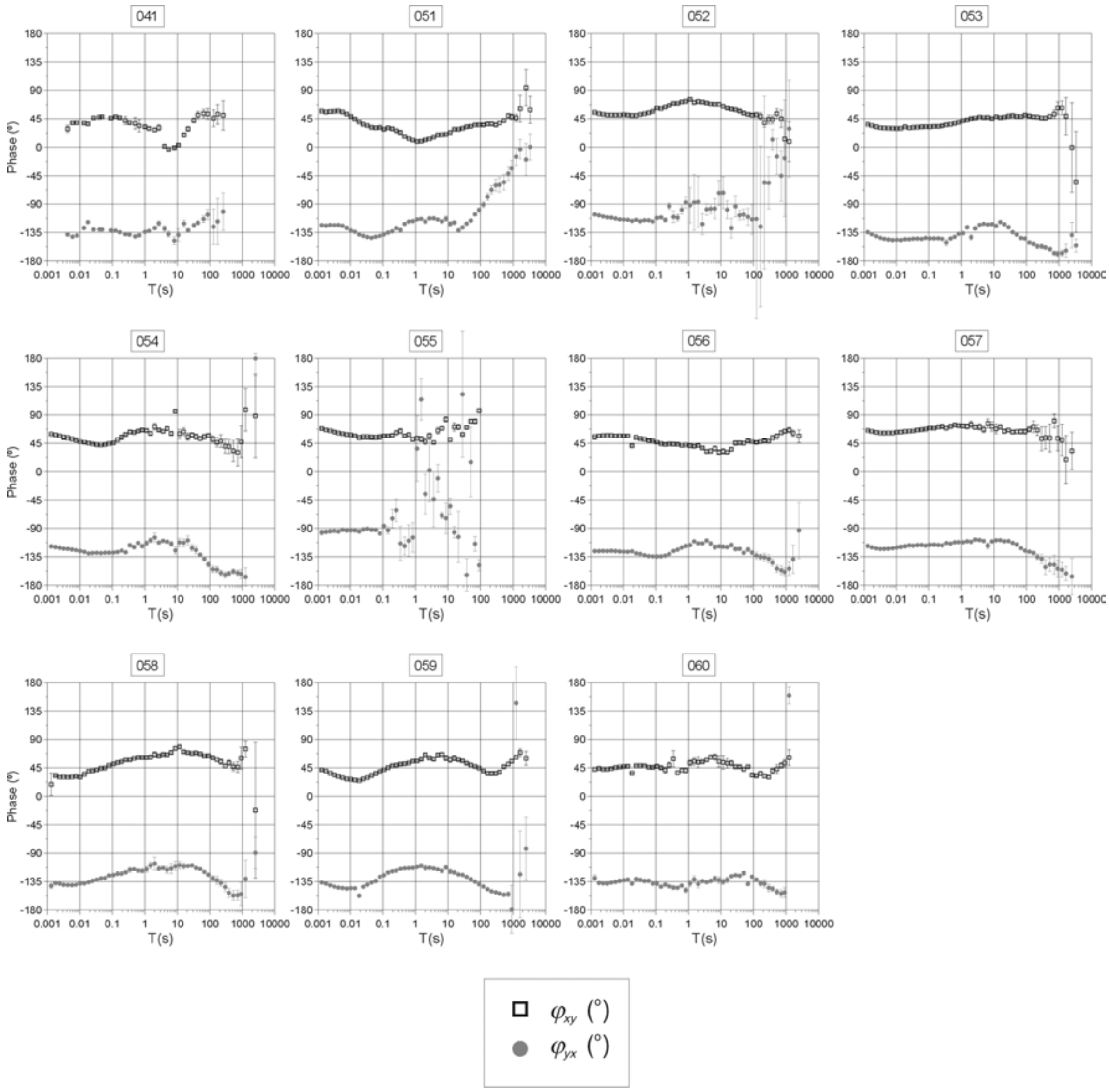

Figure D.6 (cont.)

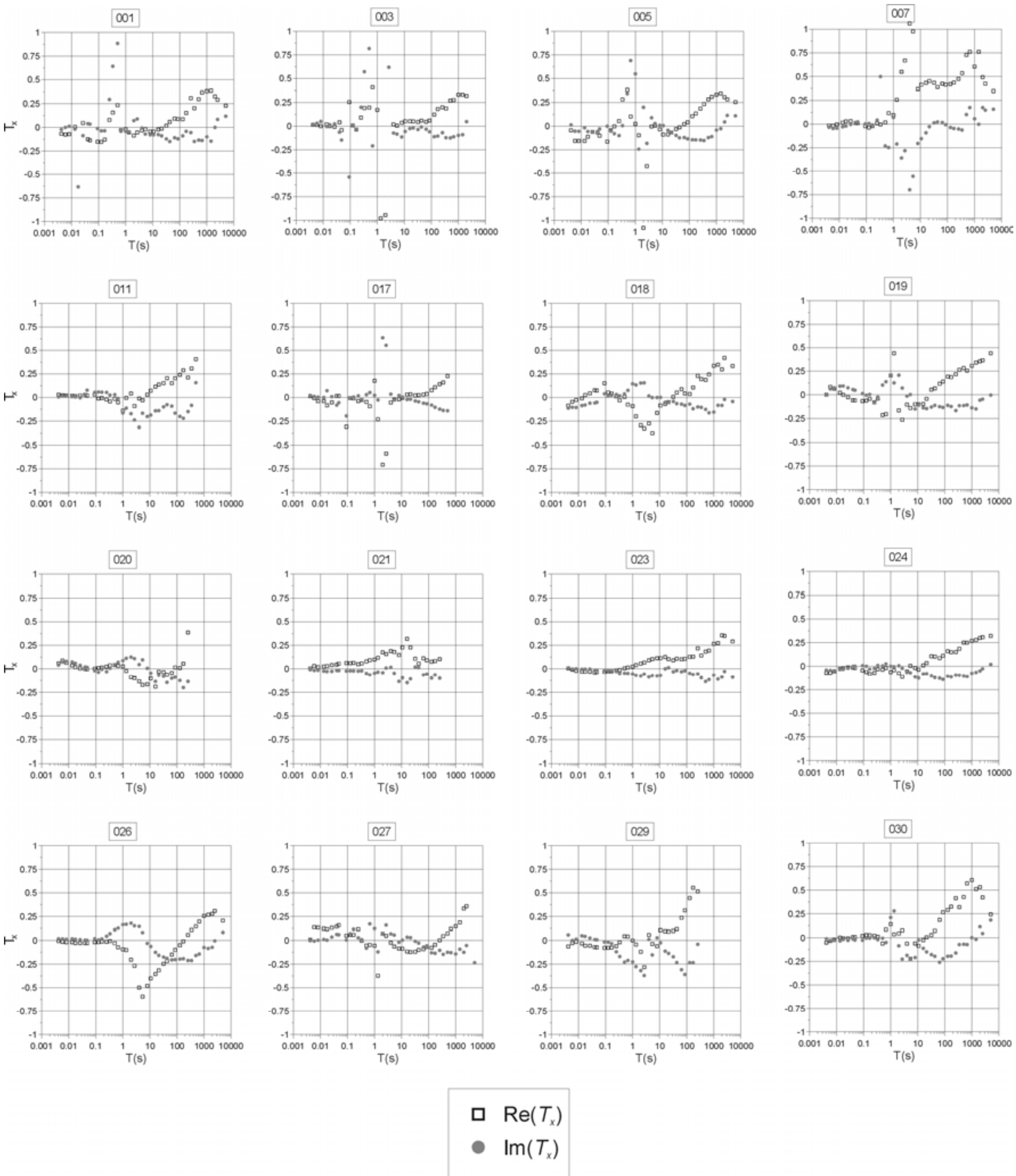

Figure D.7: Real and imaginary parts of x and y tipper components (Re(T_x), Im(T_x) and Re(T_y), Im(T_y)) for sites 001 to 030 from the Betics MT dataset in which the vertical magnetic component was registered.

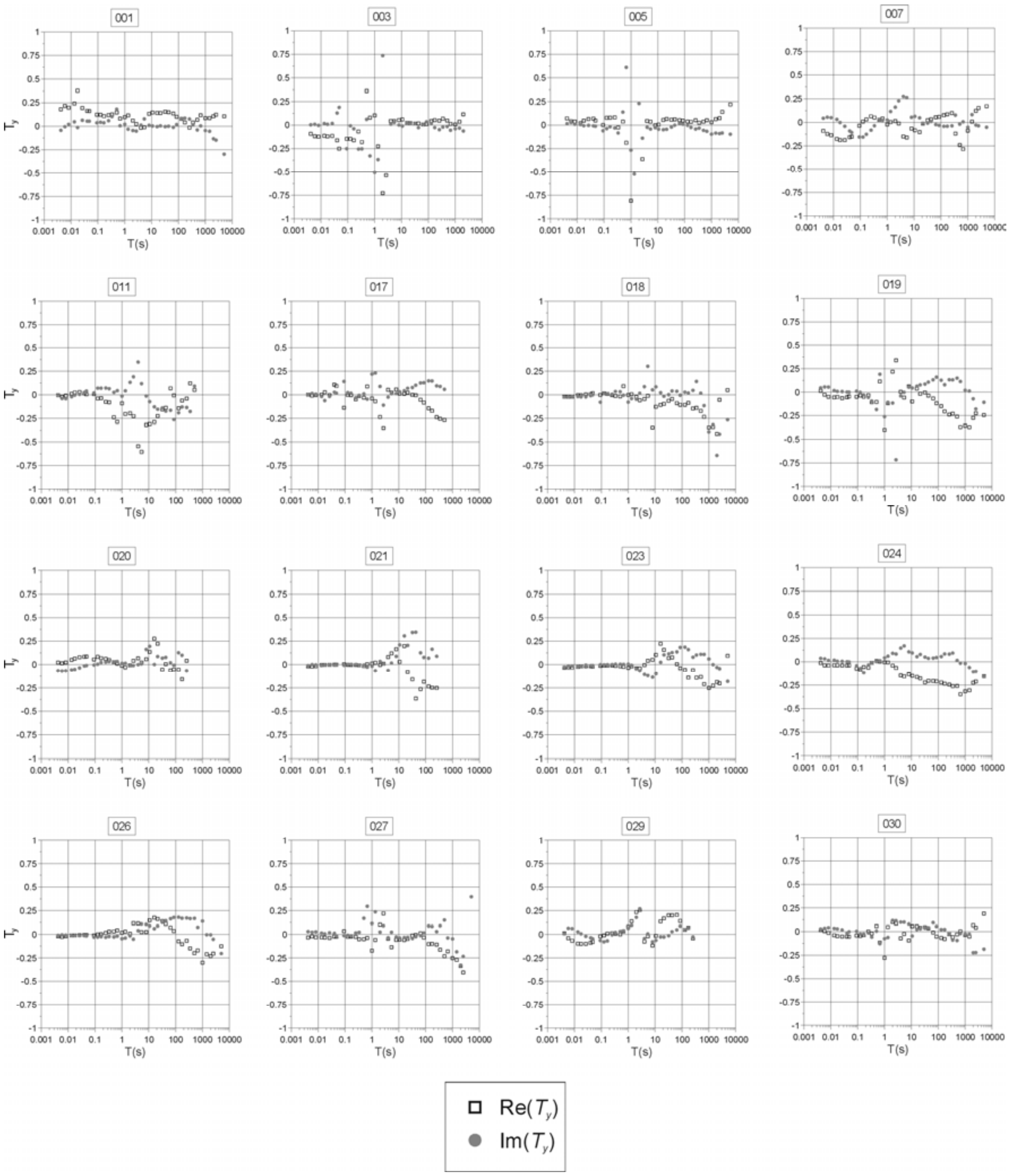

Figure D.7 (cont.)

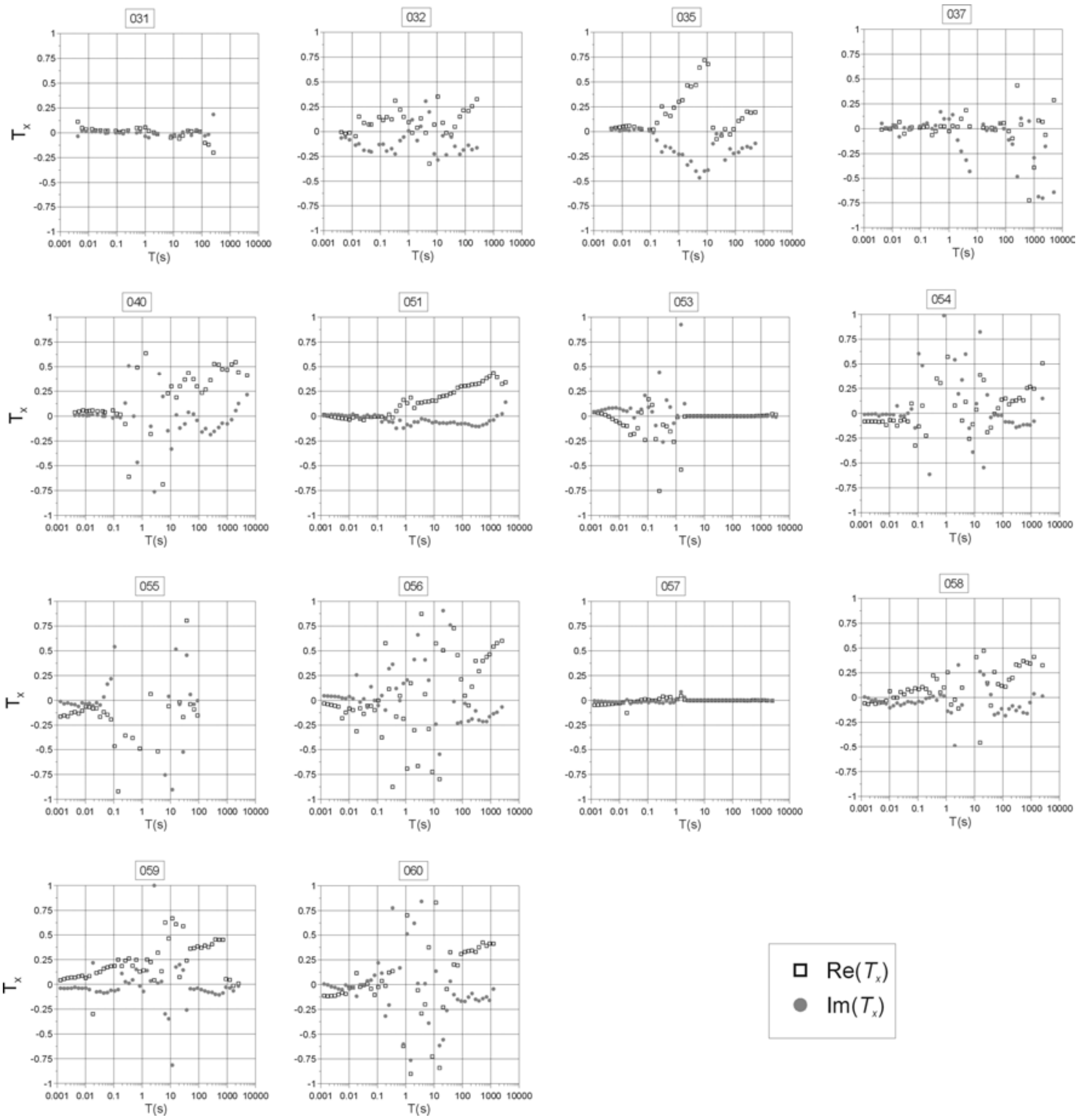

Figure D.8: Real and imaginary parts of x and y tipper components (Re(T_x), Im(T_x) and Re(T_y), Im(T_y)) for sites 031 to 060 from the Betics MT dataset in which the vertical magnetic component was registered.

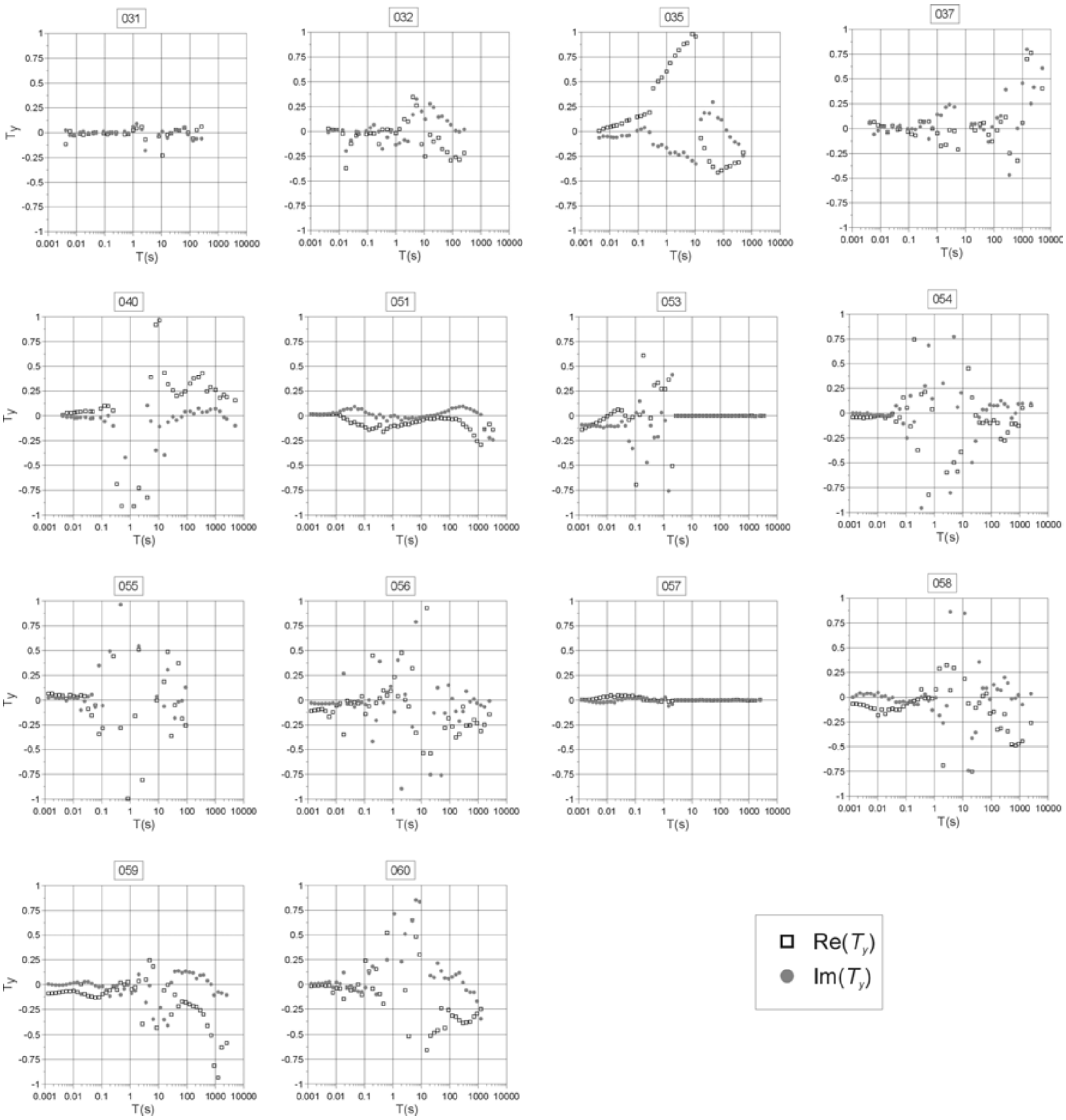

Figure D.8 (cont.)

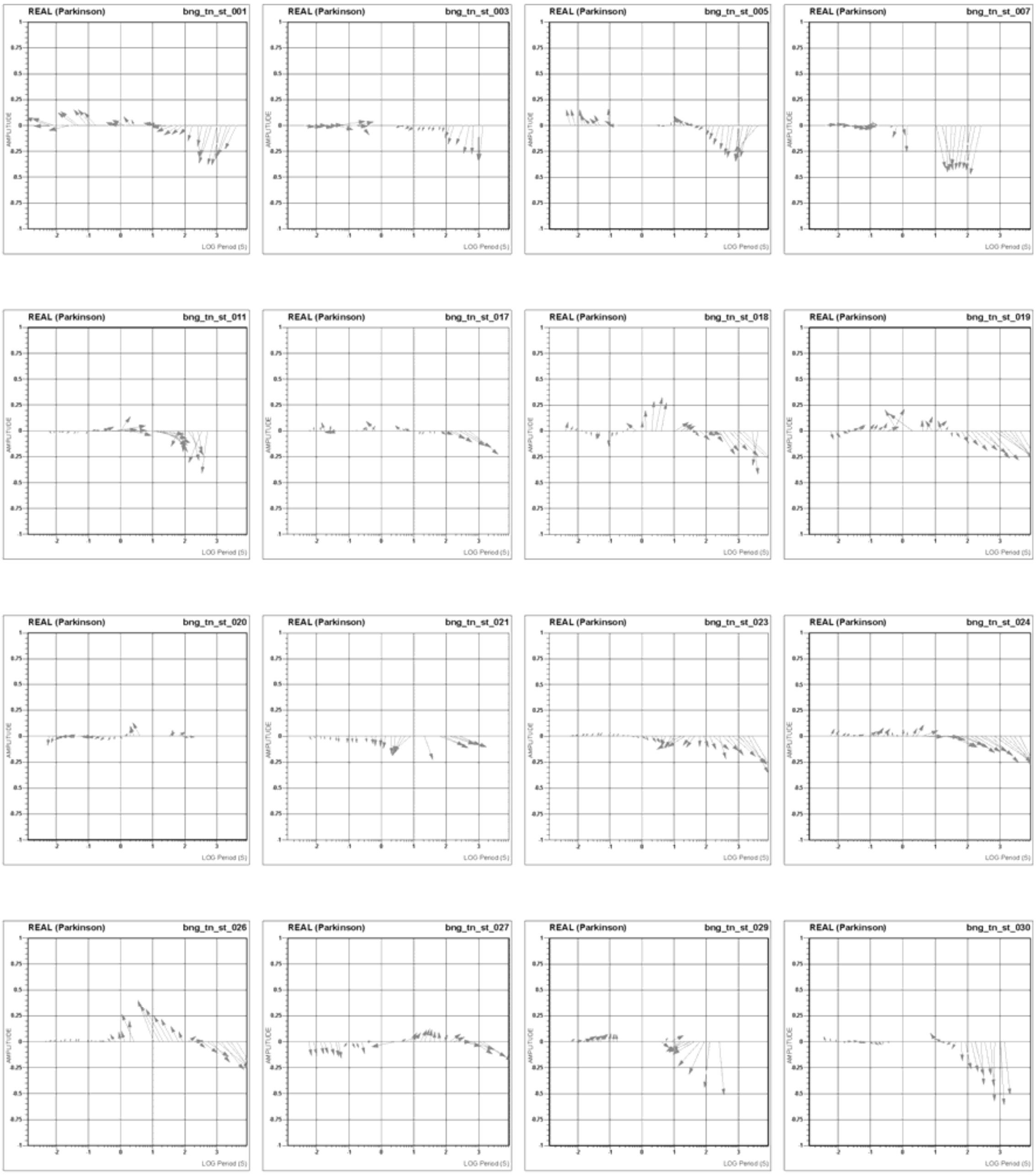

Figure D.9: Real induction arrows following Parkinson convention (inverted, i.e. pointing at conductive regions) plotted for all sites from the Betics MT dataset.

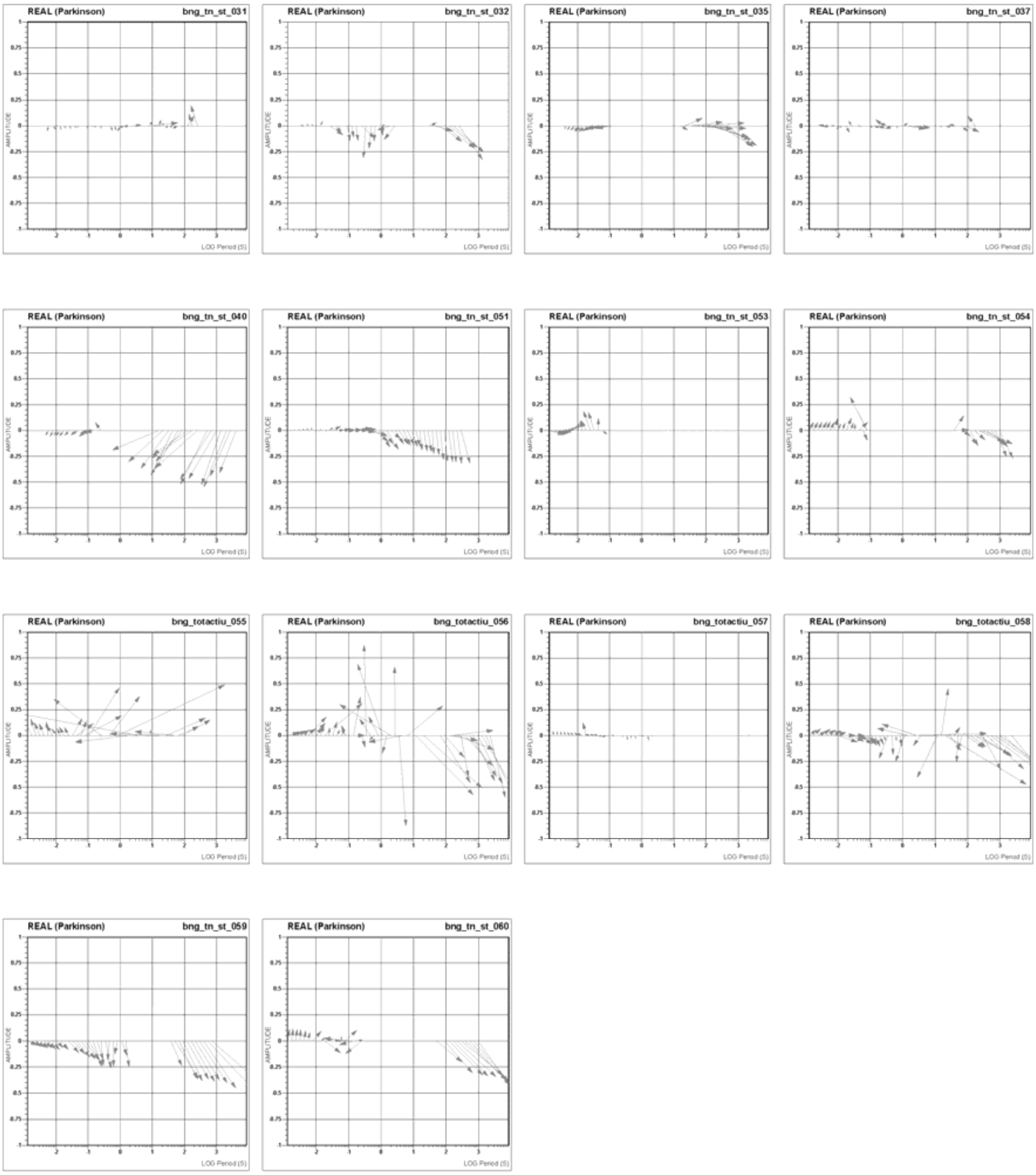

Figure D.9 (cont.)

Appendix E: Data and Model bet3D-140 Responses

The following plots display the MT responses corresponding to the Betics MT dataset, with the exception of b09, and the 3D model bet3D-140. These responses are determinant resistivity and phases (Figures E.1 to E.6) and the non-diagonal components, xy and yx, apparent resistivities and phases (Figures E.7 to E.12).

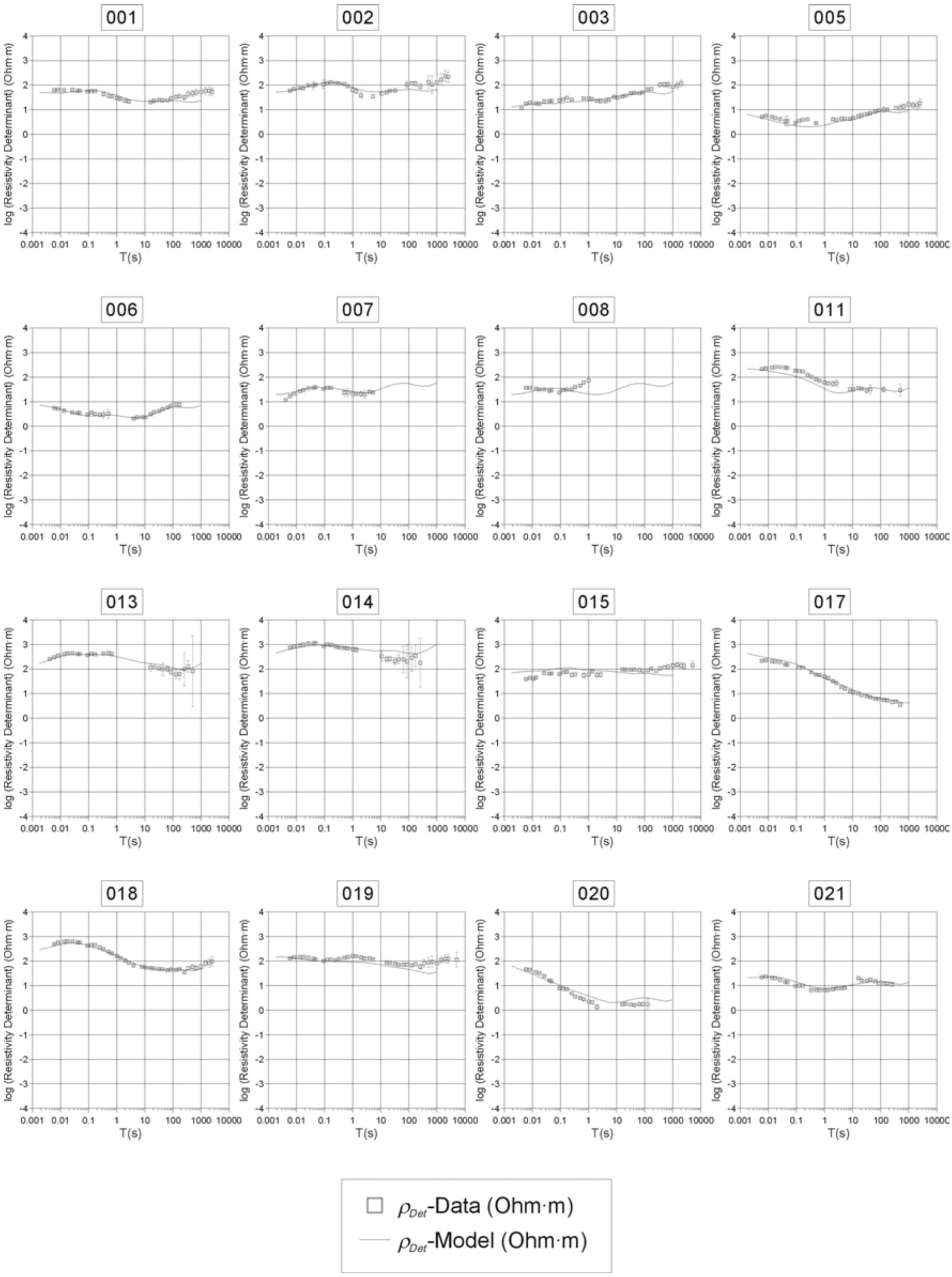

Figure E.1: Determinant resistivity data and model responses. Sites 1 to 21.

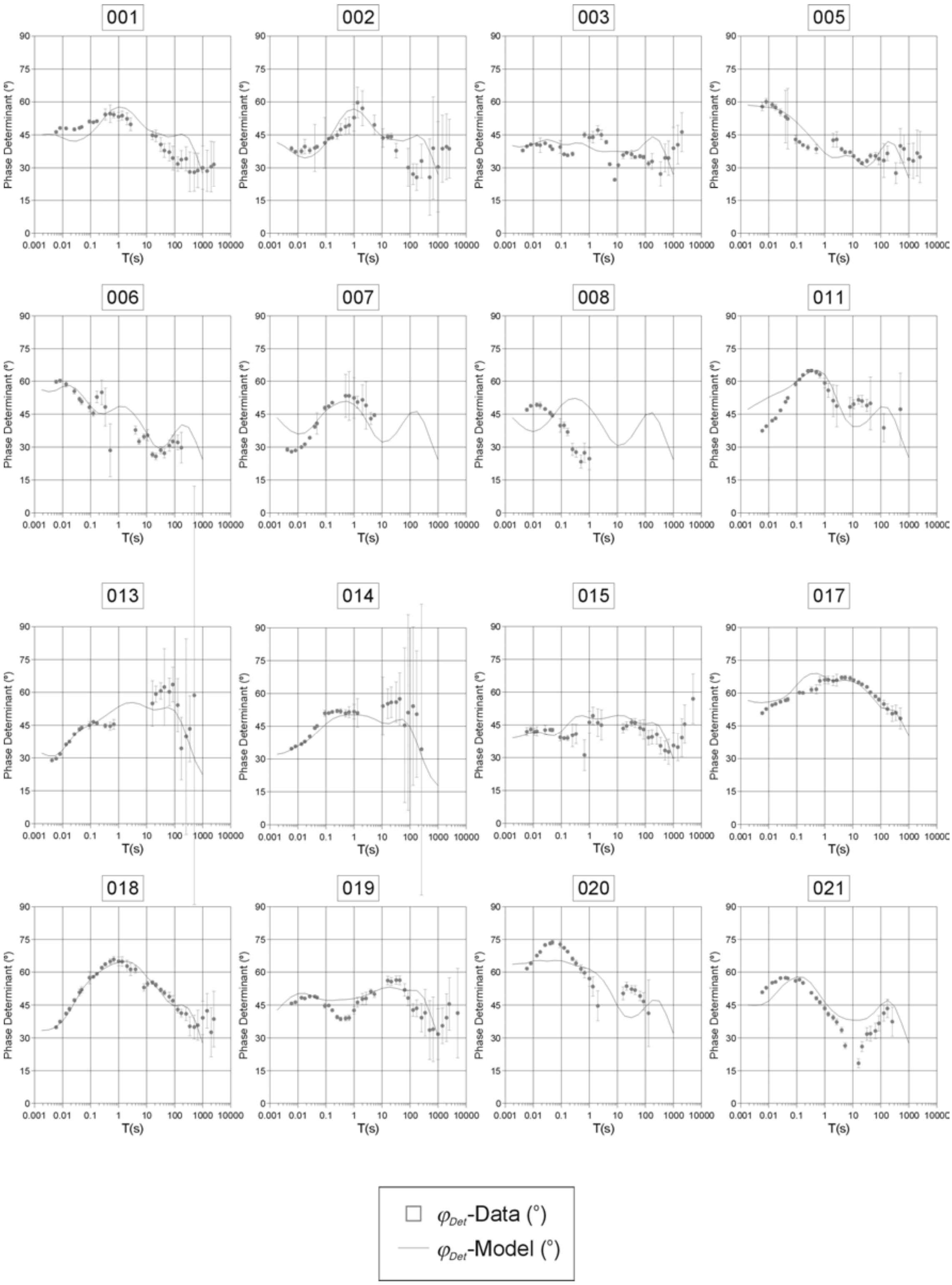

Figure E.2: Determinant phase data and model responses. Sites 1 to 21.

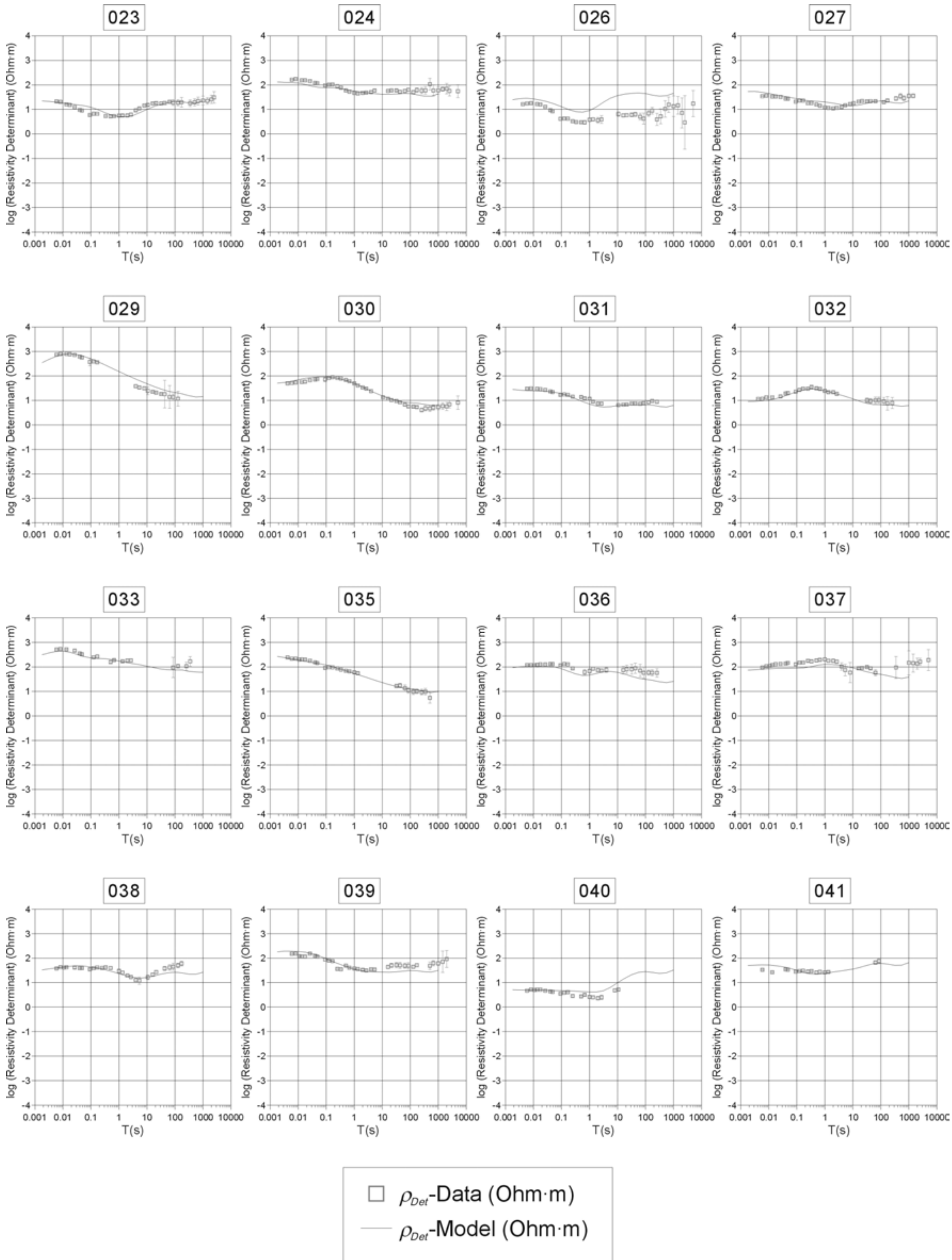

Figure E.3: Determinant resistivity data and model responses. Sites 23 to 41.

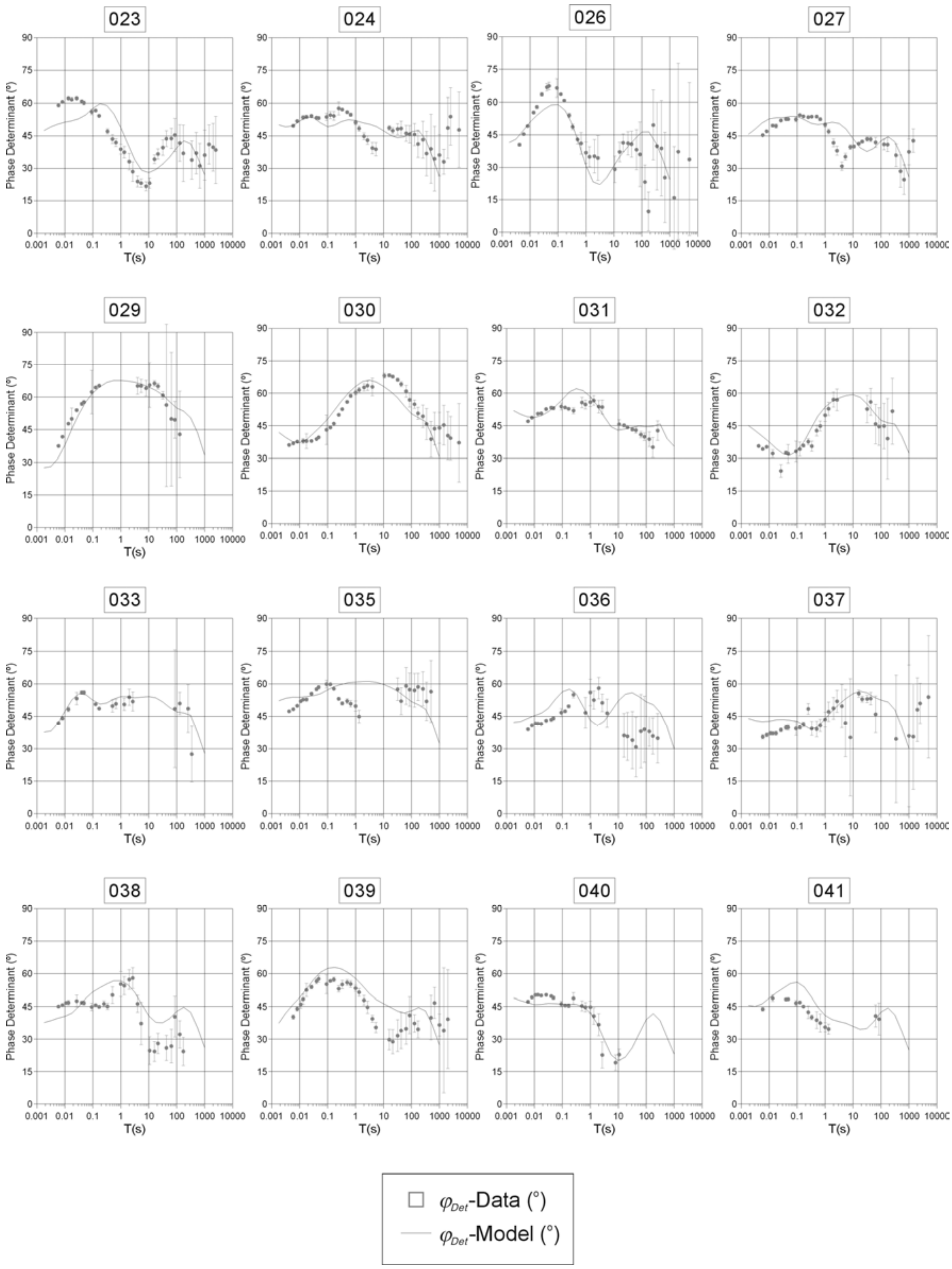

Figure E.4: Determinant phase data and model responses. Sites 23 to 41.

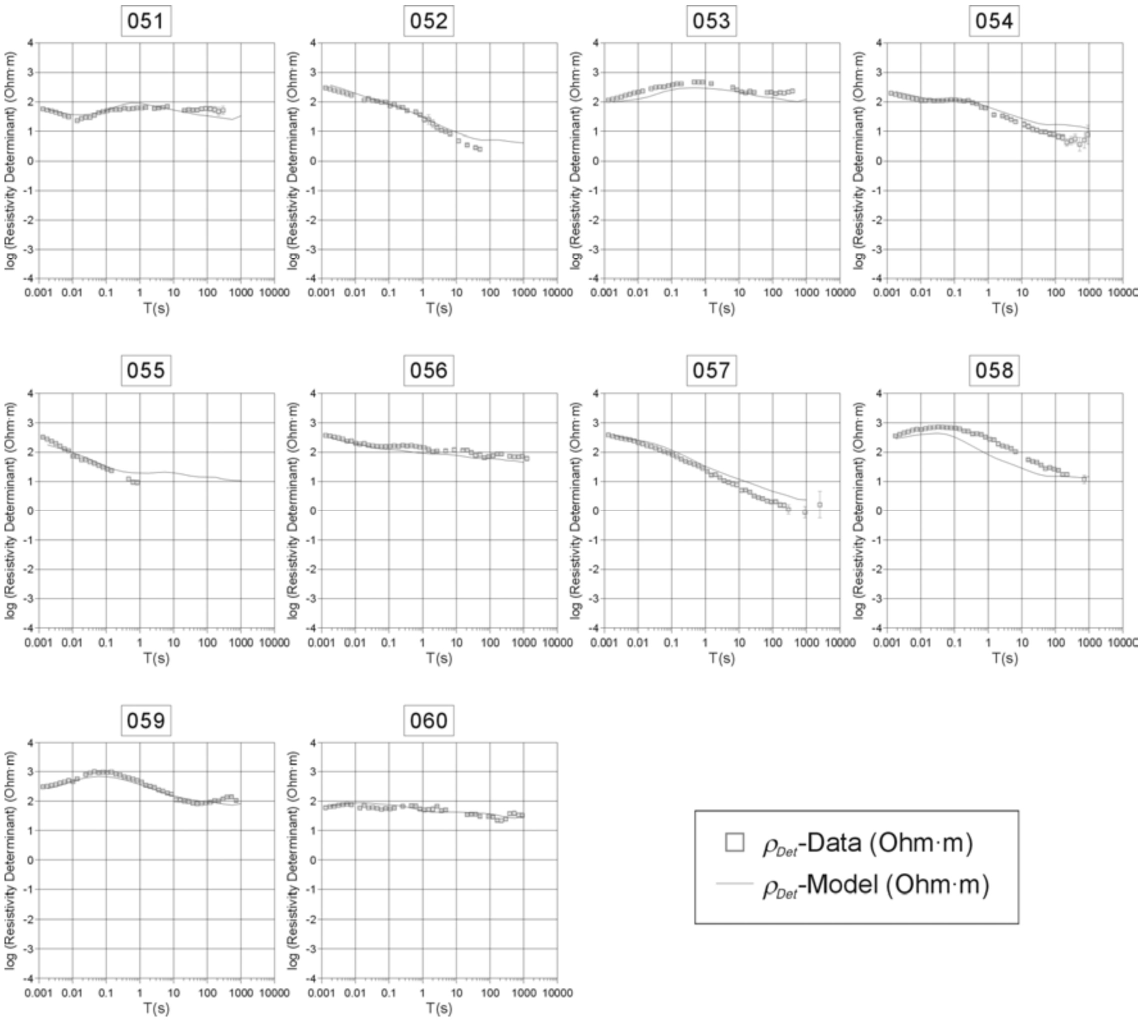

Figure E.5: Determinant resistivity data and model responses. Sites 51 to 60.

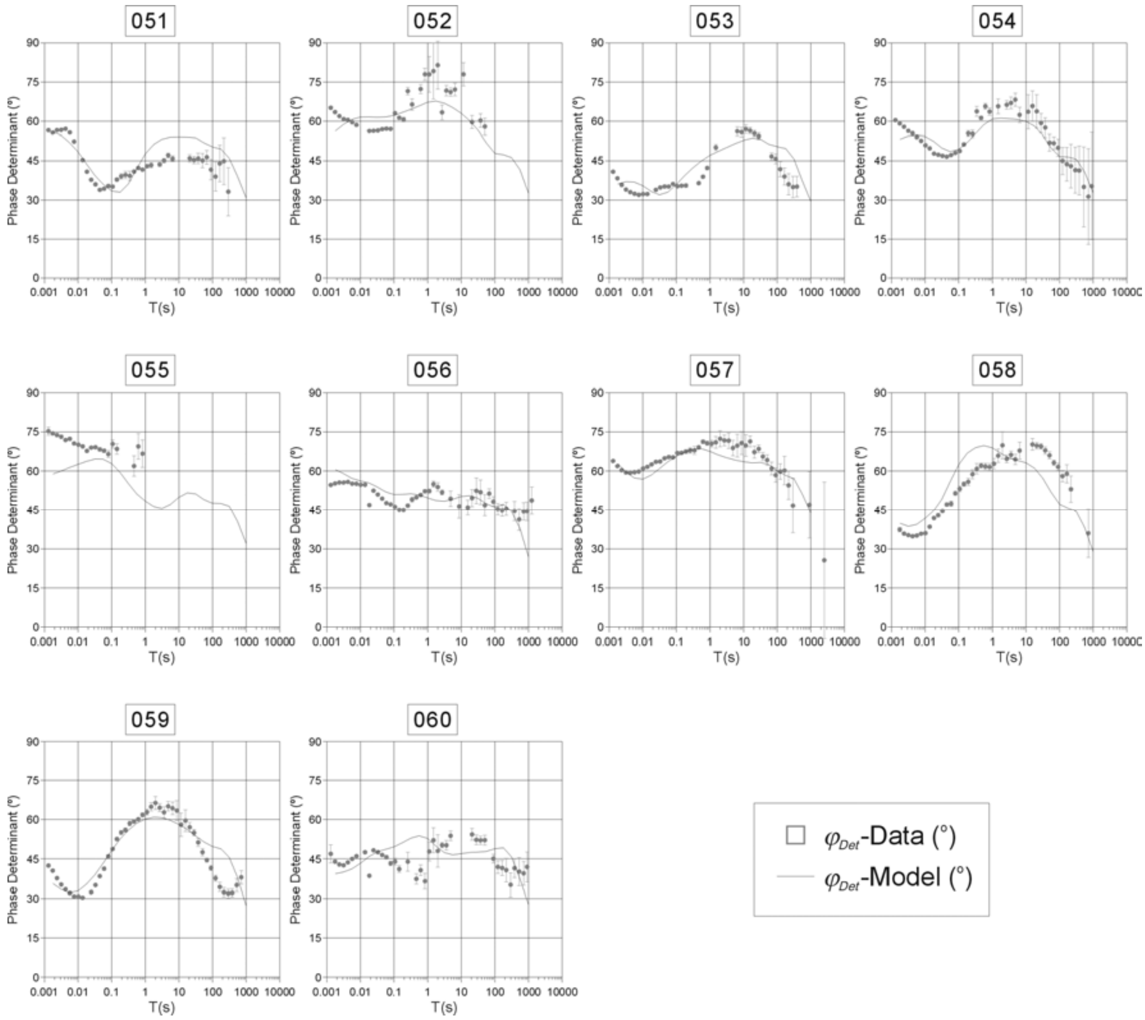

Figure E.6: Determinant phase data and model responses. Sites 51 to 60.

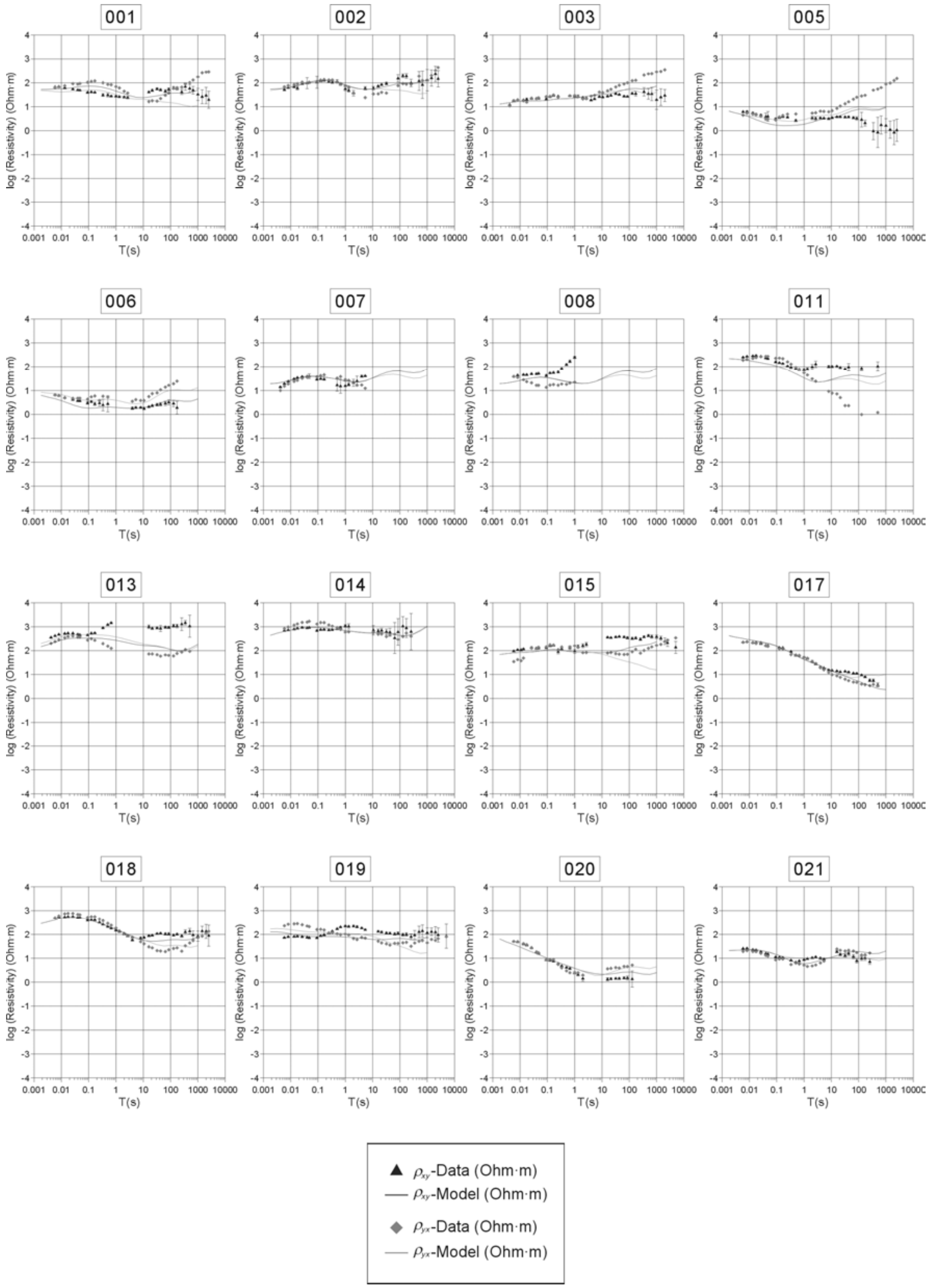

Figure E.7: xy and yx resistivity data and model responses. Sites 1 to 21.

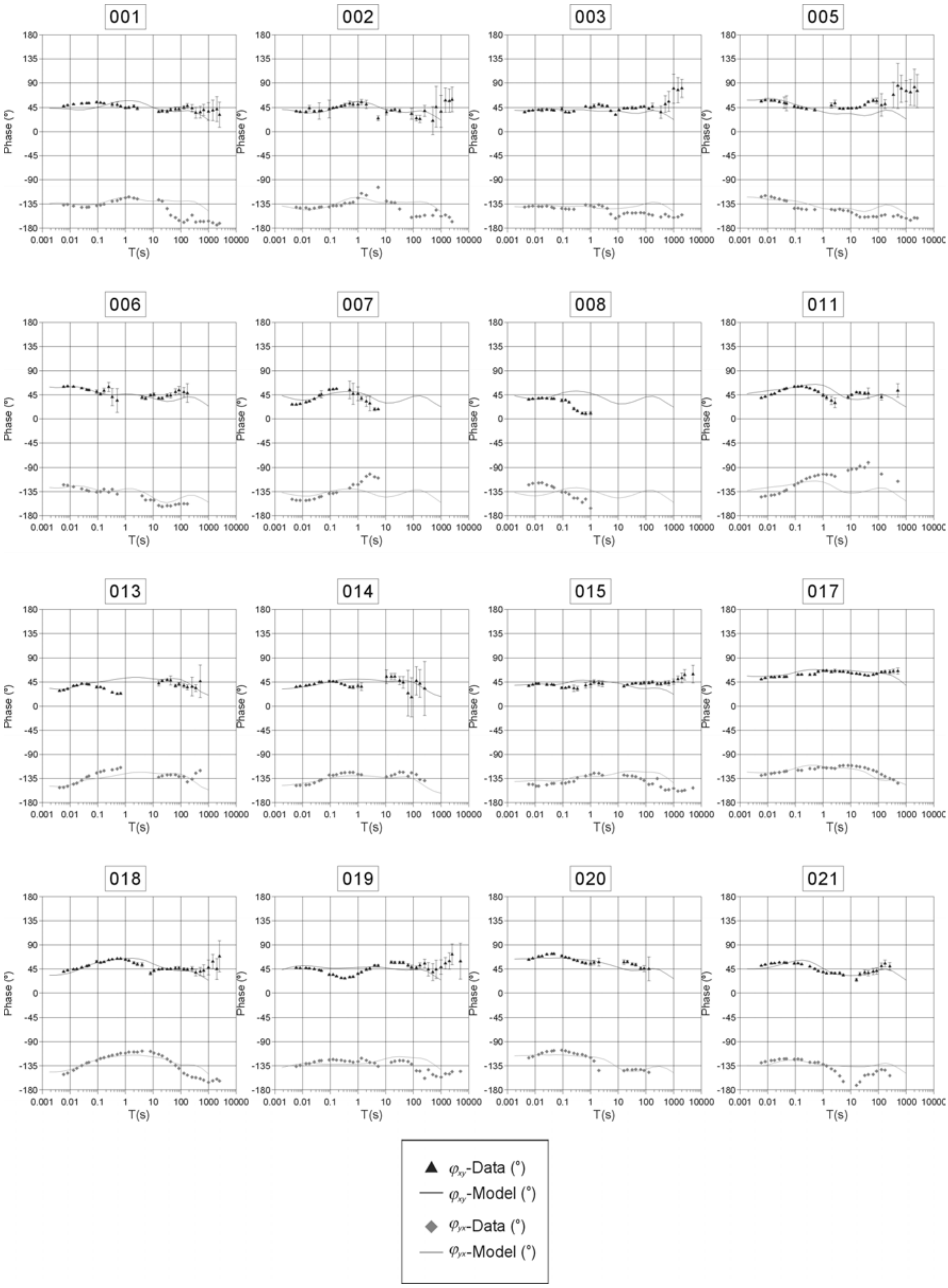

Figure E.8: xy and yx phase data and model responses. Sites 1 to 21.

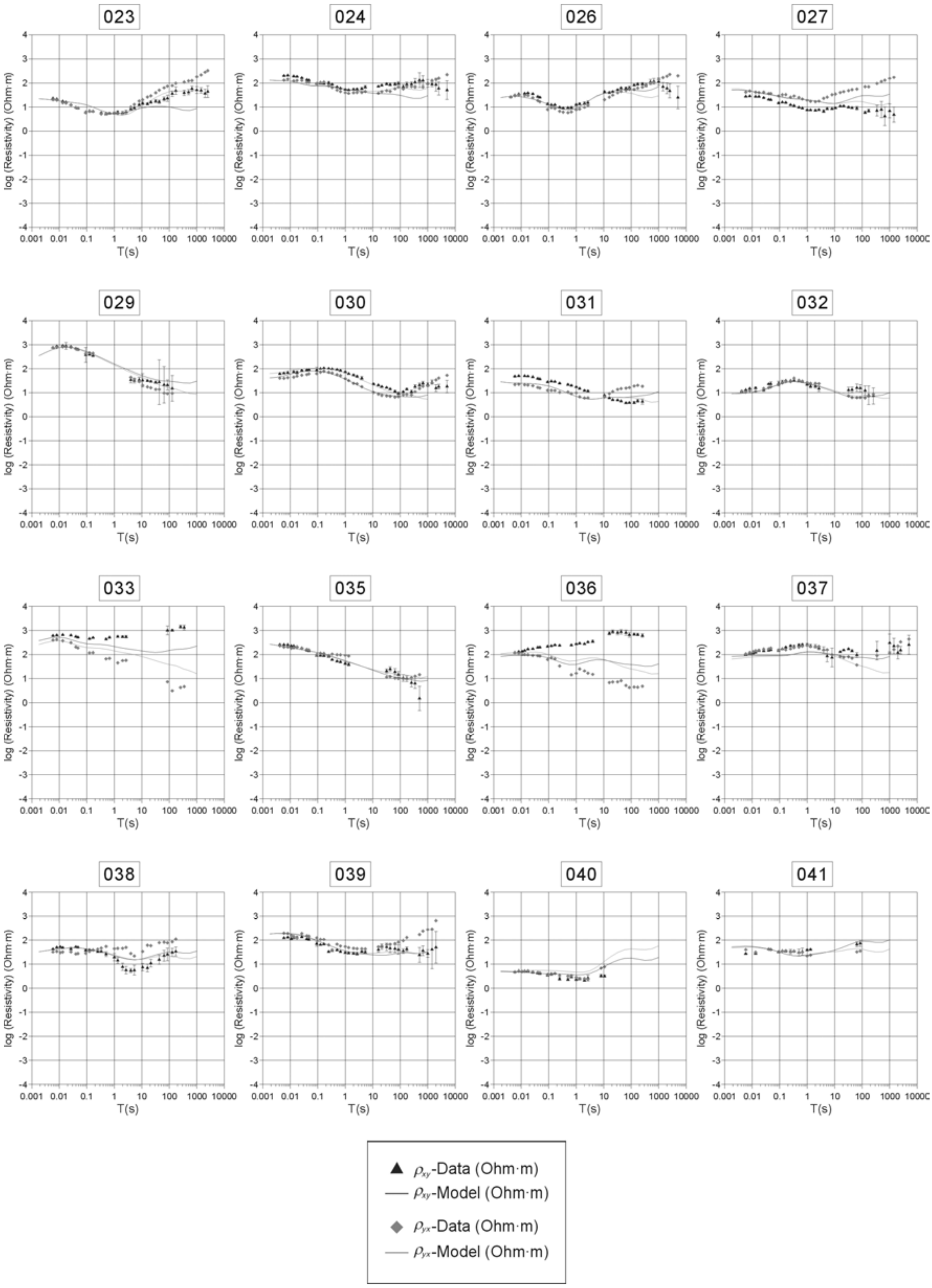

Figure E.9: xy and yx resistivity data and model responses. Sites 23 to 41.

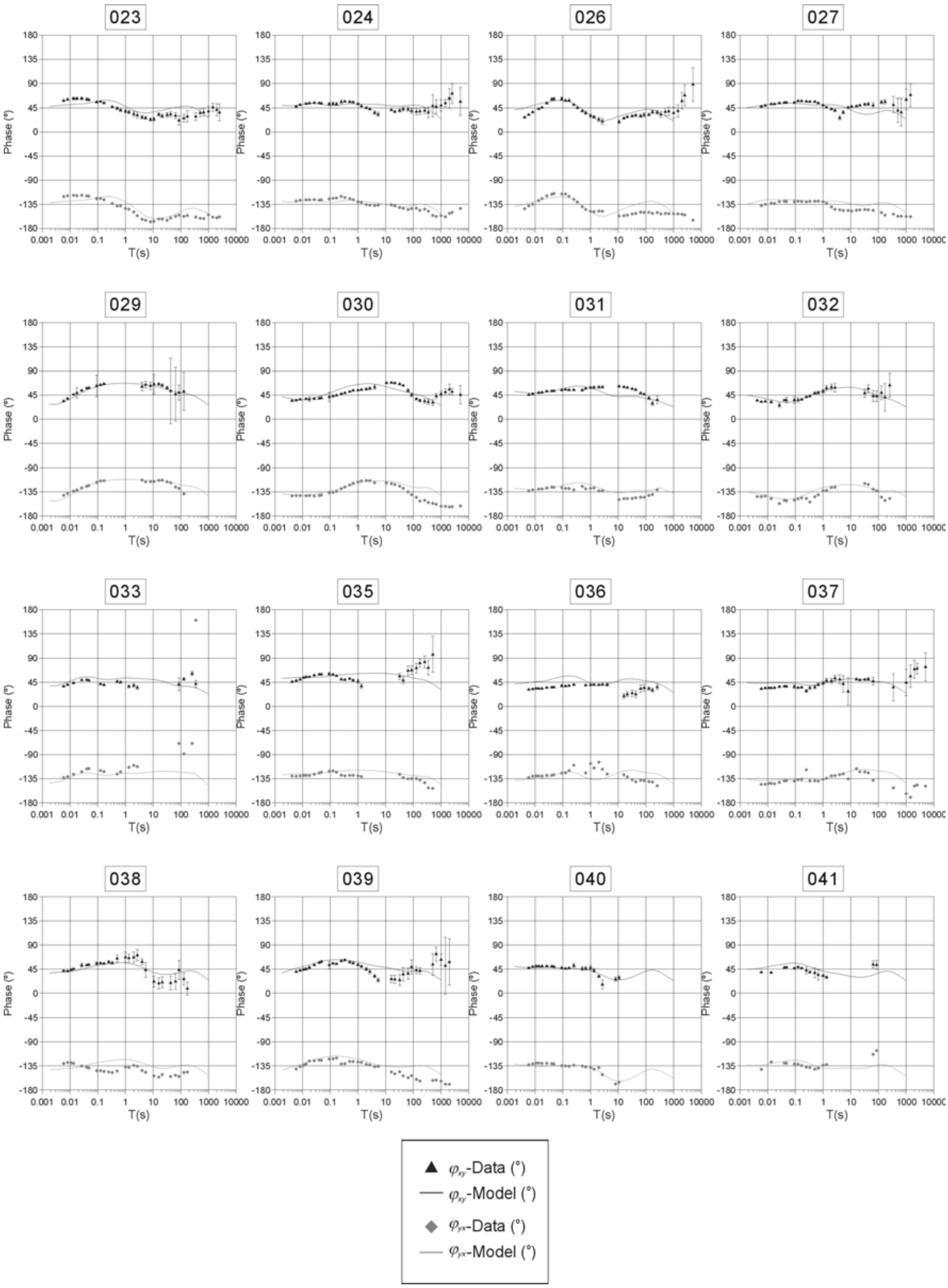

Figure E.10: xy and yx phase data and model responses. Sites 23 to 41.

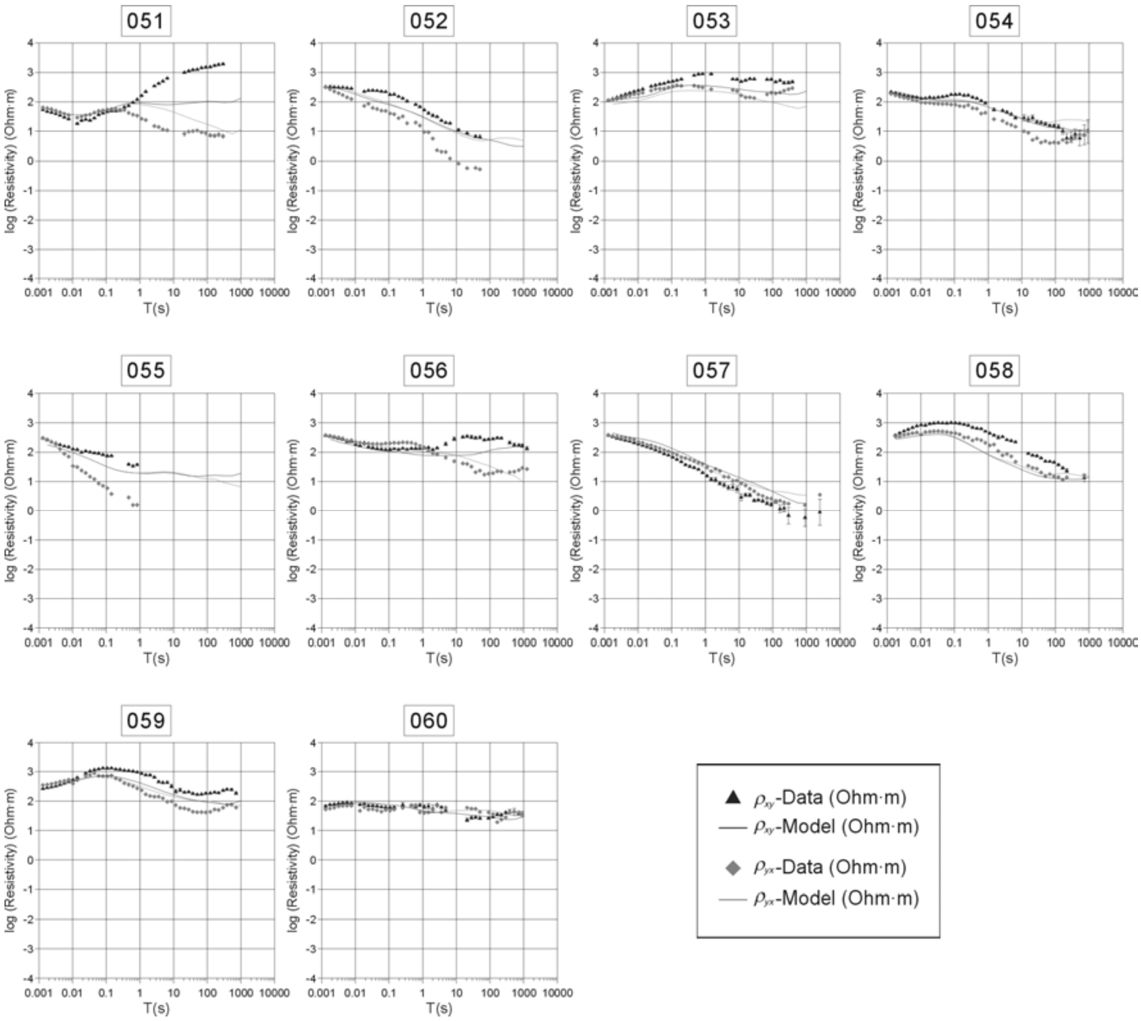

Figure E.11: xy and yx resistivity data and model responses. Sites 51 to 60.

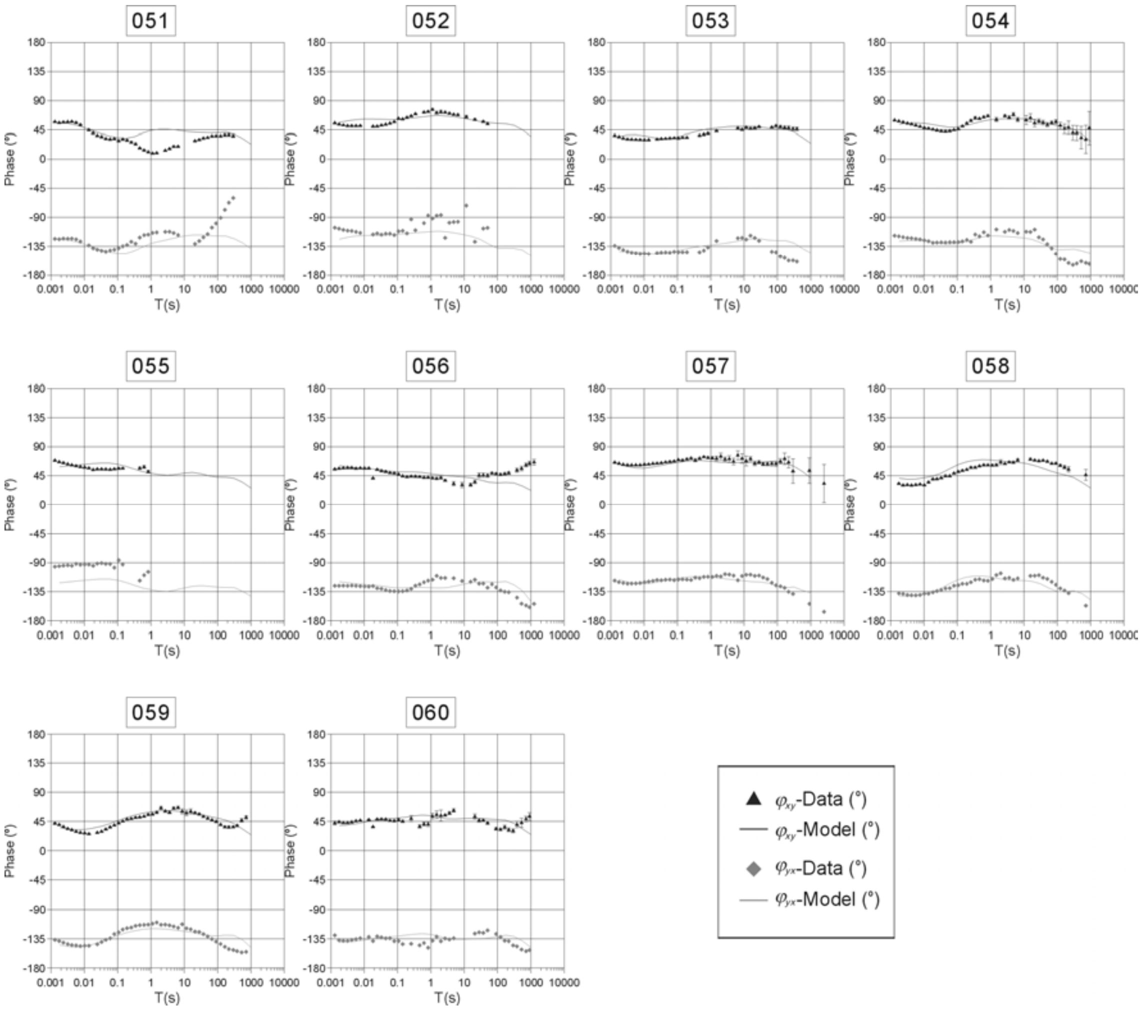

Figure E.12: xy and yx phase data and model responses. Sites 51 to 60.

Appendix F: Single Value Decomposition (SVD) of Distortion Matrix *C*

A Single Value Decomposition (SVD) of the distortion matrix was proposed by Caldwell *et al.* (2004) (equation F.2). In this work, the general expressions of this decomposition along with some particular cases were developed. The particular cases were obtained from the distortion parameters defined by Groom and Bailey (1989).

Distortion matrix:

$$C = \begin{bmatrix} C_1 & C_2 \\ C_3 & C_4 \end{bmatrix} = \frac{g}{\sqrt{1+t^2}\sqrt{1+e^2}\sqrt{1+s^2}} \begin{bmatrix} (1+s)(1-te) & (1+s)(e-t) \\ (1+s)(e+t) & (1-s)(1+te) \end{bmatrix}. \quad \text{(F.1)}$$

SVD:

$$C = R^T(\alpha_D - \beta_D) \begin{bmatrix} c_{Max} & 0 \\ 0 & c_{min} \end{bmatrix} R(\alpha_D + \beta_D) \, , \quad \text{(F.2)}$$

where:

$$c^2_{\substack{Max \\ min}} = \frac{Tr(DD^T) \pm \sqrt{Tr(DD^T)^2 - 4\det(DD^T)}}{2} = \frac{C_1^2 + C_2^2 + C_3^2 + C_4^2 \pm \sqrt{(C_1^2 + C_2^2 + C_3^2 + C_4^2)^2 - 4(C_1C_4 - C_2C_3)^2}}{2} \, , \quad \text{(F.3)}$$

$$\alpha_D = \arctan\left(\frac{e+st}{-te+s}\right)/2 \, , \quad \text{(F.4)}$$

$$\beta_D = \arctan\left(\frac{-t-se}{1-ste}\right)/2 \, . \quad \text{(F.5)}$$

Particular cases, depending on the values of t, e and s parameters:

Only twist and shear (absence of anisotropy, s=0):

$$c_{Max} = \frac{g\sqrt{1+2e+e^2+t^2+t^2e^2+2et^2}}{\sqrt{1+t^2}\sqrt{1+e^2}}, \quad \text{(F.6)}$$

$$c_{min} = \frac{g\sqrt{1-2e+e^2+t^2+t^2e^2-2et^2}}{\sqrt{1+t^2}\sqrt{1+e^2}}, \quad \text{(F.7)}$$

$$\alpha_D = \arctan\left(\frac{e}{-te}\right)/2, \quad \text{(F.8)}$$

$$\beta_D = \arctan\left(-t\right)/2. \quad \text{(F.9)}$$

Only twist (e=0, s=0):

$$c_{Max} = c_{min} = g, \quad \text{(F.10)}$$

$$\alpha_D = \arctan\left(\frac{0}{0}\right)/2 = \mathit{undefined}\,;\ \beta_D = \arctan\left(-t\right)/2. \quad \text{(F.11)}$$

The representation in this case is a circle.

Only shear (t=0, s=0):

$$c_{Max} = \frac{g(1+e)}{\sqrt{1+e^2}} \quad \text{(F.12)}$$

$$c_{Max} = \frac{g(1-e)}{\sqrt{1+e^2}} \quad \text{(F.13)}$$

$$\alpha_D = \arctan\left(\frac{1}{0}\right)/2 = 45\,\text{deg}\,;\ \beta_D = \arctan\left(0\right)/2 = 0\,\text{deg}. \quad \text{(F.14)}$$

The graphical representation corresponds to an ellipse with an azimuth of 45^{o}.

Only anisotropy (t=0, e=0):

$$c_{Max} = \frac{g(1+s)}{\sqrt{1+s^2}} \quad \text{(F.15)}$$

$$c_{Max} = \frac{g(1-s)}{\sqrt{1+s^2}} \quad \text{(F.16)}$$

$$\alpha_D = \arctan\left(\frac{0}{0}\right)/2 = \mathit{undefined}\,;\ \beta_D = \arctan\left(0\right)/2 = 0\,\text{deg}. \quad \text{(F.17)}$$

It can be represented by an ellipse aligned along x and y-axes.

These graphical descriptions obviously lead to the same used in Groom and Bailey (1989).

The Dimensionality Sudoku

	$\delta\theta$				3D			Q
1D			I				θ	3D
		Q		θ	1D			
		3D		Q				θ
	Q			I	$\delta\theta$		1D	
2D			θ					
		1D		3D	3D/ 2D			
I						Q		2D
		3D/ 2D	2D			τ		

dedicat als amants dels jocs numèrics